CLINICAL AND DIAGNOSTIC LABORATORY IMMUNOLOGY, May 2003, p. 489–491 Vol. 10, No. 3
1071-412X/03/$08.00+0 DOI: 10.1128/CDLI.10.3.489–491.2003

A Patient with Crimean-Congo Hemorrhagic Fever Serologically Diagnosed by Recombinant Nucleoprotein-Based Antibody Detection Systems

Qing Tang,[1] Masayuki Saijo,[2] Yuzhen Zhang,[3] Muer Asiguma,[3] Dong Tianshu,[3] Lei Han,[1] Bawudong Shimayi,[4] Akihiko Maeda,[2] Ichiro Kurane,[2] and Shigeru Morikawa[2]*

Second Division of Viral Hemorrhagic Fever, Institute of Infectious Disease Control and Prevention, Chinese Center for Disease Control and Prevention, Beijing 102206,[1] and Xinjiang Bachu County People's Hospital[3] and Bachu County Center for Disease Control and Prevention,[4] Bachu County, Kashi District, Xinjiang Autonomous Region, People's Republic of China, and Special Pathogens Laboratory, Department of Virology 1, National Institute of Infectious Diseases, Musashimurayama, Tokyo 208-0011, Japan[2]

Received 23 October 2002/Returned for modification 6 February 2003/Accepted 25 February 2003

We treated a male patient with Crimean-Congo hemorrhagic fever (CCHF). The diagnosis of CCHF was confirmed by reverse transcription-PCR and recombinant nucleoprotein (rNP)-based immunoglobulin G (IgG) and IgM capture enzyme-linked immunosorbent assays of serially collected serum samples. The patient was treated with intravenous ribavirin and recovered with no consequences. The study indicates that rNP-based CCHF virus antibody detection systems are useful for confirming CCHF virus infections. This case also suggests that intravenous ribavirin therapy may be promising for the treatment of CCHF patients.

Case report. We treated a patient with Crimean-Congo hemorrhagic fever (CCHF). The diagnosis of CCHF was confirmed by reverse transcription-PCR (RT-PCR) and a recombinant CCHF virus (CCHFV) nucleoprotein (rNP)-based enzyme-linked immunosorbent assay (ELISA) for detection of immunoglobulin G (IgG) to CCHFV (6). Furthermore, an IgM capture ELISA using the CCHFV rNP was used as a serological tool for the diagnosis of this patient. This patient was successfully treated by intravenous administration of ribavirin.

The patient was a 28-year-old male shepherd who lived in an area of the western part of the Xinjiang Uygur Autonomous Region, People's Republic of China, where CCHF is endemic. Taking the day on which the fever first appeared as day 1, he visited a local clinic on day 1. He spent 3 nights at home but deteriorated abruptly. He was transferred to our hospital and hospitalized on day 4. He did not know whether he had been bitten by a tick, one of the main reservoirs of CCHFV. He presented on admission with low-grade fever, unconsciousness, and severe hemorrhage from the nostrils, gingiva, skin, and gastrointestinal tract. He had anemia, and the erythrocyte count and hemoglobin level were 3.41×10^{12} cells/liter (normal range, 4.5×10^{12} to 5.9×10^{12} cells/liter) and 10.0 g/dl (normal range, 13.5 to 17.5 g/dl), respectively. Thrombocytopenia was noticed, with a platelet count of 84×10^9/liter (normal range, 150×10^9 to 400×10^9/liter). The alanine transaminase, aspartate aminotransferase, and lactate dehydrogenase levels were 173 U/liter (normal range, 5 to 40 U/liter), 216 U/liter (normal range, 5 to 40 U/liter), and 268 U/liter (normal range, 114 to 240 U/liter), respectively, suggesting liver dysfunction. Mild hyperbilirubinemia, hypoproteinemia, and hypoalbuminemia were also present. Renal function was preserved. The patient was intravenously administered ribavirin (0.6 g/dose twice a day, 2-h drip infusion) from day 4 to 11. The symptoms improved gradually, and the patient recovered with no consequences.

Blood samples were drawn for diagnostic tests on days 1, 5, and 9. The blood sample drawn on day 1 was collected at the initial clinic visit and was brought to our hospital. Serum was separated and kept at −20°C until use. A nested RT-PCR was performed for amplification of the viral genome. Viral RNA was extracted from 200 μl of serum with a High Pure Viral RNA Kit (Roche Diagnostics GmbH, Mannheim, Germany) in accordance with the manufacturer's instructions. The primers were modified from those reported by other investigators (4) in accordance with the nucleotide sequence of Chinese CCHFV isolate 8402 (GenBank accession no. AJ010649). Five microliters of purified RNA was added to the Ready to Go RT-PCR mixture (0.5-ml tubes; Amersham Pharmacia Biotech Inc., Piscataway, N.J.) as a template, and then the primer set of 50 pmol each of CCHF/F2C (5′-TGGATACTTTCACAAACTC-3′) and CCHF/R3 (5′-GACAAATTCCCTGCACCA-3′) and an appropriate amount of water were added to the tube. The RT-PCR was performed in accordance with the manufacturer's instructions. The tube was kept at 42°C for 30 min for the RT reaction. The reverse transcriptase was then heat inactivated at 95°C for 5 min. The PCR conditions were as follows: 35 cycles of denaturation at 95°C for 30 s, annealing at 52°C for 30 s, and elongation at 72°C for 30 s, followed by an additional elongation at 72°C for 5 min. For the nested PCR, 1 μl of the first-round PCR product was added to a 0.5-ml Ready to Go PCR tube (Amersham Pharmacia Biotech Inc.) as a template and then 50 pmol each of primers CCHF/F3C (5′-GAGTGT GCCTGGGTTAGCTC-3′) and CCHF/R2C (5′-GACATTAC

* Corresponding author. Mailing address: Special Pathogens Laboratory, Department of Virology 1, National Institute of Infectious Diseases, 4-7-1 Gakuen, Musashimurayama, Tokyo 208-0011, Japan. Phone: 81-42-561-0771, ext. 791. Fax: 81-42-561-2039. E-mail: morikawa@nih.go.jp.

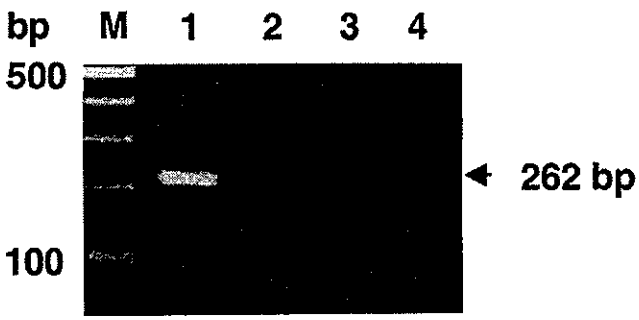

FIG. 1. Results of the nested RT-PCR assay of serum samples serially collected from the patient. Lanes: M, 100-bp markers; 1, 2, 3, and 4, day 1, 5, and 9 serum and negative control samples, respectively. A PCR product of the expected size (262 bp) was amplified only from the day 1 serum sample.

AATTTCGCCAGG-3') and an appropriate amount of water were added to the PCR tube. The second-round PCR was performed under the same conditions as described above. The PCR product was separated by electrophoresis in a 2% agarose gel and visualized by staining with ethidium bromide. The expected size of the PCR product was 262 bp.

IgG antibodies to CCHFV were detected by a CCHFV rNP-based IgG ELISA (6). IgM antibodies to CCHFV were detected by an IgM capture ELISA with the same antigen. The ELISA plate was coated with goat anti-human IgM antibody (μ chain specific; Zymed Laboratories Inc., South San Francisco, Calif.) at an approximate concentration of 100 ng/well at 4°C overnight. After the plate was washed with phosphate-buffered saline solution containing 0.05% Tween 20 (T-PBS), it was treated with the blocking reagent, 200 μl of T-PBS containing 5% skim milk (T-PBS-M) per well, at 37°C for 1 h. The plate was washed with T-PBS, and the top four and bottom four wells of the plate were inoculated with heat-inactivated test serum samples (100 μl/well), which were diluted twofold from 1:50 to 1:400 with T-PBS-M. The plate was incubated at 37°C for 1 h. After being washed with T-PBS, the top four wells of the plate were inoculated with the purified CCHFV rNP in T-PBS-M (100 μl/well) at a concentration of 1 μg/ml while the bottom four wells were also inoculated with T-PBS-M as a negative control. After being washed with T-PBS, all of the wells were inoculated with anti-CCHFV rNP rabbit serum at a dilution of 1:1,000 (6). After being washed with T-PBS, the plate was inoculated with goat anti-rabbit IgG antibody labeled with horseradish peroxidase (Zymed Laboratories Inc.) at a dilution of 1:1,000. The plate was washed with T-PBS, 2,2'-azino-di[3-ethylbenzthiazolin sulfate (6)] (ABTS) solution (Roche Diagnostics GmbH) was added to each well, and the plate was incubated at 37°C for 30 min. The optical density at 405 nm (OD_{405}) was measured with a reference of 490 nm. The OD_{405} was adjusted by subtracting the OD_{405} of the non-antigen-inoculated well from that of the corresponding antigen-inoculated well. The cutoff value for the IgG ELISA at a dilution of 1:400 was defined as reported previously (6). The cutoff value that determined IgM positivity or negativity was calculated as the average plus 3 standard deviations of serum samples collected from 48 subjects with no history of CCHFV infection.

The viral genome was detected by nested RT-PCR in the day 1 serum sample but not in those from days 5 and 9 (Fig. 1). Neither IgM nor IgG antibodies to CCHFV were detected in the day 1 serum sample. On the other hand, IgM and IgG were both detected in the serum samples collected on days 5 and 9 (Table 1). The titers were higher on day 9 than on day 5.

TABLE 1. IgG and IgM antibodies to CCHFV detected by ELISAs in serum samples drawn sequentially

Class of antibodies and dilution	OD_{405} of samples and antibody[a]			Cutoff[b]
	Day 1	Day 5	Day 9	
IgM				
1:50	0.000	2.692	2.709	ND[c]
1:100	0.020	2.672	2.711	0.205
1:200	0.044	2.528	2.767	ND
1:400	0.040	1.606	2.001	ND
IgG				
1:100	0.075	0.924	1.882	ND
1:400	0.031	0.486	0.972	0.213
1:1,600	0.000	0.152	0.384	ND
1:6,400	0.000	0.045	0.132	ND

[a] The OD_{405} values shown here were adjusted as described in the text.
[b] Cutoff values for IgM and IgG responses were defined at dilutions of 1:100 and 1:400, respectively, as described in the text. According to these cutoff values, both the IgM and IgG responses were demonstrated in the serum samples drawn on days 5 and 9 but not in the day 1 sample.
[c] ND, not determined.

The virological and immunological status of CCHFV infection was closely followed by nested RT-PCR and the ELISAs. We previously reported the CCHFV rNP-based antibody detection systems (5, 6). In the present study, we used a CCHFV rNP-based IgM capture ELISA along with an IgG ELISA. We applied these assays to the serum samples serially collected from the patient. The results suggest that both the CCHFV rNP-based IgG ELISA and the IgM capture ELISA are useful for the diagnosis of CCHF. We believe that this is the first case of CCHF serologically diagnosed by CCHFV rNP-based antibody detection systems.

Ribavirin, an anti-RNA virus agent, has been reported to have an inhibitory effect on the replication of CCHFV in vitro and in vivo (2, 7, 9). There have been several reports on ribavirin therapy for CCHF (1, 3, 8). However, the efficacy of ribavirin for CCHF has not yet been proved. Oral ribavirin was used for postexposure prophylaxis of CCHFV infection with promising results, but its efficacy was not formally assessed (8). The patient in the present study was treated by intravenous administration of ribavirin. To our knowledge, this is the first case report of a CCHF patient treated with intravenous ribavirin therapy. The previous reports, along with the present study, suggest that ribavirin is a promising drug for the treatment of CCHF.

REFERENCES

1. **Fisher-Hoch, S. P., J. A. Khan, S. Rehman, S. Mirza, M. Khurshid, and J. B. McCormick.** 1995. Crimean Congo-haemorrhagic fever treated with oral ribavirin. Lancet 346:472–475.
2. **Huggins, J. W.** 1989. Prospects for treatment of viral hemorrhagic fevers with ribavirin, a broad spectrum antiviral drug. Rev. Infect. Dis. ii:S750–S761.
3. **Papa, A., B. Bozovi, V. Pavlidou, E. Papadimitriou, M. Pelemis, and A. Antoniadis.** 2002. Genetic detection and isolation of Crimean-Congo hemorrhagic fever virus, Kosovo, Yugoslavia. Emerg. Infect. Dis. 8:852–854.
4. **Rodriguez, L. L., G. O. Maupin, T. G. Ksiazek, P. E. Rollin, A. S. Khan, T. F.**

Schwarz, R. S. Lofts, J. F. Smith, A. M. Noor, C. J. Peters, and S. T. Nichol. 1997. Molecular investigation of a multisource outbreak of Crimean-Congo hemorrhagic fever in the United Arab Emirates. Am. J. Trop. Med. Hyg. **57**:512–518.

5. **Saijo, M., Q. Tang, M. Niikura, A. Maeda, T. Ikegami, C. Prehaud, I. Kurane, and S. Morikawa.** 2002. An immunofluorescence technique for detection of immunoglobulin G antibodies to Crimean-Congo hemorrhagic fever virus using HeLa cells expressing recombinant nucleoprotein. J. Clin. Microbiol. **40**:372–375.
6. **Saijo, M., Q. Tang, M. Niikura, A. Maeda, T. Ikegami, C. Prehaud, I. Kurane, and S. Morikawa.** 2002. Recombinant nucleoprotein-based enzyme-linked immunosorbent assay for detection of immunoglobulin G to Crimean-Congo hemorrhagic fever virus. J. Clin. Microbiol. **40**:1587–1591.
7. **Tignor, G. H., and C. A. Hanham.** 1993. Ribavirin efficacy in an in vivo model of Crimean-Congo hemorrhagic fever virus (CCHF) infection. Antivir. Res. **22**:309–325.
8. **Van de Wal, B. W., J. R. Joubert, P. J. van Eeden, and J. B. King.** 1985. A nosocomial outbreak of Crimean-Congo haemorrhagic fever at Tygerberg Hospital. Part IV. Preventive and prophylactic measures. S. Afr. Med. J. **68**:729–732.
9. **Watts, D. M., M. A. Ussery, D. Nash, and C. J. Peters.** 1989. Inhibition of Crimean-Congo hemorrhagic fever viral infectivity yields in vitro by ribavirin. Am. J. Trop. Med. Hyg. **41**:581–585.

CLINICAL AND DIAGNOSTIC LABORATORY IMMUNOLOGY, July 2003, p. 552–557 Vol. 10, No. 4
1071-412X/03/$08.00+0 DOI: 10.1128/CDLI.10.4.552–557.2003

Antigen Capture Enzyme-Linked Immunosorbent Assay for Specific Detection of Reston Ebola Virus Nucleoprotein

Tetsuro Ikegami,[1,2] Masahiro Niikura,[1]† Masayuki Saijo,[1] Mary E. Miranda,[3] Alan B. Calaor,[3] Marvin Hernandez,[3] Luz P. Acosta,[3] Daria L. Manalo,[3] Ichiro Kurane,[1] Yasuhiro Yoshikawa,[2] and Shigeru Morikawa[1]*

Special Pathogens Laboratory, Department of Virology 1, National Institute of Infectious Diseases, Musashimurayama, Tokyo 208-0011,[1] and Department of Biomedical Science, Graduate School of Agricultural and Life Sciences, The University of Tokyo, Bunkyo-ku, Tokyo 113-8657,[2] Japan, and Veterinary Research Department, Research Institute for Tropical Medicine, Department of Health, Muntinlupa City 1770, Philippines[3]

Received 21 February 2003/Returned for modification 3 April 2003/Accepted 5 May 2003

Antigen capture enzyme-linked immunosorbent assay (ELISA) is one of the most useful methods to detect Ebola virus rapidly. We previously developed an antigen capture ELISA using a monoclonal antibody (MAb), 3-3D, which reacted not only to the nucleoprotein (NP) of Zaire Ebola virus (EBO-Z) but also to the NPs of Sudan (EBO-S) and Reston Ebola (EBO-R) viruses. In this study, we developed antigen capture ELISAs using two novel MAbs, Res2-6C8 and Res2-1D8, specific to the NP of EBO-R. Res2-6C8 and Res2-1D8 recognized epitopes consisting of 4 and 8 amino acid residues, respectively, near the C-terminal region of the EBO-R NP. The antigen capture ELISAs using these two MAbs detected the EBO-R NP in the tissues from EBO-R-infected cynomolgus macaques. The antigen capture ELISAs using Res2-6C8 and Res2-1D8 are useful for the rapid detection of the NP in EBO-R-infected cynomolgus macaques.

The family *Filoviridae* includes the genera *Marburgvirus* and *Ebolavirus*. The genus *Ebolavirus* has four species: *Zaire Ebola virus* (EBO-Z), *Sudan Ebola virus* (EBO-S), *Côte-d'Ivoire Ebola virus* (EBO-CI), and *Reston Ebola virus* (EBO-R) (6, 11, 13, 27, 34). Ebola virus has a negative-stranded RNA genome that encodes nucleoprotein (NP), P protein (VP35), matrix protein (VP40), glycoprotein (GP), an NP that influences the synthesis of viral mRNA (VP30), a protein associated with the membrane (VP24), and RNA-dependent RNA polymerase (L) (6, 26, 27, 34).

Cynomolgus macaques infected with EBO-R, which is thought to be endemic in the Philippines, were exported to the United States and Italy (2–4, 12, 16, 25, 30, 38). As with other species of Ebola virus, EBO-R causes fatal illness in nonhuman primates (7, 17), while symptomatic EBO-R infection has not been reported in humans (3, 4, 25, 38).

The origin in nature of Ebola virus remains a mystery; however, humans can be infected by close contact with patients (34, 36, 37). Rapid laboratory diagnosis of Ebola hemorrhagic fever is important for preventing the expansion of infection. Virus isolation (19, 23, 34), transmission electron microscopy (19, 23, 34), immunohistochemistry (39), reverse transcription-PCR (RT-PCR) (2, 21, 35), the fluorogenic 5′ nuclease assay (10), and antigen capture enzyme-linked immunosorbent assay (ELISA) (18, 29) have been used for the laboratory diagnosis of Ebola virus infection. Since the viral load in the blood reaches extremely high levels in Ebola virus infections (5, 7, 17, 31), the detection of Ebola antigens by antigen capture ELISA is suitable as a method of laboratory diagnosis (18, 29).

Monoclonal antibodies (MAbs) that discriminate Ebola virus species have been reported (28). However, an antigen capture ELISA that discriminates Ebola virus species has not been reported. In the present study, we developed antigen capture ELISAs using two novel MAbs to the NP specific to EBO-R. The ELISAs will be a useful tool for rapid discrimination of EBO-R infection from those by other Ebola virus species, especially in monkey quarantine or field studies.

MATERIALS AND METHODS

Cell culture. P3/Ag568 was used as the parental cell line for hybridomas. The cells were maintained in RPMI 1640 (Gibco BRL, Rockville, Md.) supplemented with 10% fetal bovine serum and antibiotics (streptomycin and penicillin; Gibco BRL). Hypoxanthine-aminopterin-thymidine supplement (HAT) (Gibco BRL) was added to the medium for the selection of hybridomas according to the manufacturer's instructions. Hypoxanthine-thymidine supplement (HT) (Gibco BRL) was added to the medium to switch the medium from HAT to RPMI 1640.

Clinical specimens. Livers (monkey no. 2882 and 2877), spleens (monkey no. 2877, 2882, and 2885), and sera (monkey no. 2866 and 2612), which were collected from EBO-R-infected cynomolgus macaques during the EBO-R outbreak in the Philippines in 1996 (14, 25) and kept frozen at −80C, were used in the study. EBO-R-NP antigens or genomic RNA were detected in these samples by antigen capture ELISA using 3-3D (29), immunohistochemistry (14), or RT-PCR using primers RES-Nf2 (5′-TGAGCTCCGGAAGAAGGACGGTGT-3′) and RES-Nr2 (5′-ACCATCATGTGTCCAACTGATTGC-3′). Five liver specimens and 79 serum specimens from EBO-R-noninfected cynomolgus macaques were used as the negative controls. Liver and spleen tissues were homogenized at approximately 10% (wt/vol) in phosphate-buffered saline (PBS) containing 0.05% Tween 20, 1% Triton X-100, and 5% nonfat milk (Triton–milk–PBS-T). After centrifugation at 15,800 × *g* for 10 min, the supernatants were used in the experiments. Sera were diluted with Triton–milk–PBS-T and used in the experiments.

Preparation of histidine-tagged Ebola virus rNPs (His-EBO-R-NP and His-EBO-Z-NP) for antigen capture ELISA. Recombinant NPs (rNP) of EBO-R (His-EBO-R-NP) and EBO-Z (His-EBO-Z-NP) were prepared to be the anti-

* Corresponding author. Mailing address: Special Pathogens Laboratory, Department of Virology 1, National Institute of Infectious Diseases, 4-7-1 Gakuen, Musashimurayama, Tokyo 208-0011, Japan. Phone: 81-42-561-0771, ext. 791. Fax: 81-42-561-2039. E-mail: morikawa@nih.go.jp.

† Present address: USDA-ARS Avian Disease and Oncology Laboratory, East Lansing, MI 48823.

TABLE 1. Primers used for epitope mapping recognized by Res2-6C8 and Res2-1D8

Primer	Sequence (5′ to 3′)[a]	Template of reaction
R635f	CAAGGATCCGAAGACCCTGATATC	pGEX-ΔNP$_{631-739}$
R636f	TTGGGATCCGACCCTGATATCGGTCAATC	cDNA of EBO-R
R637f	TTGAATGGATCCCCTGATATCGGT	pGEX-ΔNP$_{631-739}$
R638f	AATGAAGGATCCGATATCGGTCAA	pGEX-ΔNP$_{631-739}$
Mu639f	TGAAGACCCTGATTAAGGTCAATCAAAGT	pGEX-ΔNP$_{631-739}$
Mu639r	ACTTTGATTGACCTTAATCAGGGTCTTCA	pGEX-ΔNP$_{631-739}$
Mu640f	AGACCCTGATATCTAACAATCAAAGTCTA	pGEX-ΔNP$_{631-739}$
Mu640r	TAGACTTTGATTGTTAGATATCAGGGTCT	pGEX-ΔNP$_{631-739}$
Mu641f	CCCTGATATCGGTTAATCAAAGTCTATGC	pGEX-ΔNP$_{631-739}$
Mu641r	GCATAGACTTTGATTAACCGATATCAGGG	pGEX-ΔNP$_{631-739}$
Mu642f	TGATATCGGTCAATAAAAGTCTATGCAAA	pGEX-ΔNP$_{631-739}$
Mu642r	TTTGCATAGACTTTTATTGACCGATATCA	pGEX-ΔNP$_{631-739}$
Mu643f	TATCGGTCAATCATAATCTATGCAAAAAT	pGEX-ΔNP$_{631-739}$
Mu643r	ATTTTTGCATAGATTATGATTGACCGATA	pGEX-ΔNP$_{631-739}$
Mu644f	CGGTCAATCAAAGTAAATGCAAAAATTAG	pGEX-ΔNP$_{631-739}$
Mu644r	CTAATTTTTGCATTTACTTTGATTGACCG	pGEX-ΔNP$_{631-739}$

[a] *Bam*HI restriction site is underlined. Introduced stop codon is in boldface.

gens in antigen capture ELISA. The recombinant baculoviruses, which expressed His-EBO-R-NP (referred to as *Ac* [*Autographa californica*]-His-EBO-R-NP) or His-EBO-Z-NP (referred to as *Ac*-His-EBO-Z-NP), were produced as described previously (15, 33). *Ac*-His-EBO-R-NP or *Ac*-His-EBO-Z-NP was grown in Tn5 insect cells as reported previously (24). Tn5 cells infected with the recombinant baculoviruses were washed twice with PBS after 3 days of culture at 26°C and then incubated for 15 min in PBS containing 1% NP-40. After sonication for 1 min, the lysates were used in the experiments.

Preparation of MAbs. MAbs were prepared as described previously (29). Briefly, BALB/c mice were subcutaneously immunized with His-EBO-R-NP together with Freund complete adjuvant (Becton Dickinson, Franklin Lakes, N.J.) and boosted subcutaneously three times with IMJECT-ALUM (Pierce, Rockford, Ill.) at 2-week intervals. Three days after the last immunization, the spleens were removed, and the spleen cells were fused with P3/Ag568 cells by using polyethylene glycol 4000 (catalog no. 4030-035; Gibco BRL) according to the manufacturer's instructions. The supernatants of the hybridoma cells were screened in an immunoglobulin G (IgG) ELISA (29) with His-EBO-R-NP as an antigen. Crude hybridomas were isolated from ELISA-positive wells, and the hybridoma clones were established by the limiting dilution method. MAbs were purified from the culture supernatants with a MAb Trap GII antibody purification kit (Amersham Pharmacia Biotech, Little Chalfont, United Kingdom) according to the manufacturer's instructions. The isotypes of the MAbs were determined with a mouse MAb isotyping kit from Gibco BRL.

Preparation of polyclonal antibodies. Rabbit antisera to the glutathione *S*-transferase (GST)-tagged EBO-R NP C-terminal half (amino acids [aa] 360 to 739) (GST-EBO-R-ΔNP) (15) and to His-EBO-Z-NP (32, 33) were prepared as described previously. Briefly, rabbits were immunized four times subcutaneously with GST-EBO-R-ΔNP or His-EBO-Z-NP together with IMJECT-ALUM (Pierce). Serum was obtained 7 days after the last immunization.

IFA. Indirect immunofluorescence assays (IFAs) using HeLa cells expressing the entire NPs of EBO-R or EBO-Z were performed as described previously (15, 32). IFA slides coated with Vero E6 cells infected with EBO-S and gamma irradiated were kindly supplied by the Centers for Disease Control and Prevention, Atlanta, Ga. The well of the slide was spotted with 20 μl of each MAb at a concentration of 100 ng/μl, and the slides were incubated under humidified conditions at 37°C for 1 h. After being washed with PBS, the slides were reacted with fluorescein isothiocyanate-conjugated goat anti-mouse IgG (H+L) antiserum (catalog no. 62-6511; Zymed Laboratories, Inc., South San Francisco, Calif.) at a dilution of 1:100. The slides were washed with PBS and examined for the staining pattern under a fluorescent microscope.

Epitope mapping with GST-truncated EBO-R rNP fusions. A series of truncated EBO-R rNPs were prepared to determine the epitopes recognized by Res2-6C8 and Res2-1D8. Table 1 shows the primers used for the construction of the peptides. A truncated EBO-R NP corresponding to aa 631 to 739 was prepared as follows. PCR using the primers RES-N8F and RES-N8R (29) was performed to amplify the corresponding region of EBO-R cDNA. The PCR fragment was subcloned into a pGEX-2T vector (Amersham Pharmacia Biotech) to construct pGEX-ΔNP$_{631-739}$. The insert sequences were confirmed to be identical to the originals. Then the GST-tagged truncated EBO-R NP was expressed in *Escherichia coli* (BL-21 strain) and purified by glutathione Sepharose 4B column chromatography according to the manufacturer's instructions (Amersham Pharmacia Biotech). PCR was also performed with the forward primers R635f, R636f, R637f, and R638f and a reverse primer, RES-N8R. As described above, each of the truncated EBO-R NPs corresponding to aa 635 to 739, 636 to 739, 637 to 739, and 638 to 739 was expressed and purified. The plasmids to express the truncated EBO-R NP corresponding to aa 631 to 638, 631 to 639, 631 to 640, 631 to 641, 631 to 642, and 631 to 643 were constructed by replacing a corresponding codon with a stop codon by site-directed mutagenesis of pGEX-ΔNP$_{631-739}$ using the primer pairs Mu639f/Mu639r, Mu640f/Mu640r, Mu641f/Mu641r, Mu642f/Mu642r, Mu643f/Mu643r, and Mu644f/Mu644r according to the manufacturer's instructions (QuikChange site-directed mutagenesis kit; Stratagene, La Jolla, Calif.). Each of the truncated EBO-R NPs was expressed and purified as described above. Then, the reactivity of Res2-6C8 and Res2-1D8 to truncated EBO-R rNPs was examined by IgG ELISA.

Antigen capture ELISA. Antigen capture ELISA was performed as described previously (29). Briefly, a microtiter plate (Becton Dickinson) was coated with purified MAbs (100 ng per well in 100 μl of PBS) overnight at 4°C. The three MAbs Res2-6C8, Res2-1D8, and 3-3D were used as the capture antibodies in the assay. MAb 3-3D was prepared against EBO-Z NP and was previously reported to detect the NPs of EBO-Z, EBO-R, and probably EBO-S in the antigen capture ELISA (29). After washing the plates three times with PBS containing 0.05% Tween 20 (PBS-T), 200 μl of PBS-T containing 5% nonfat milk (milk–PBS-T) was added to the wells for blocking for 1 h at 37°C. The milk–PBS-T was then removed, and 100 μl of the samples was added to the wells, which were then incubated for 1 h at 37°C. Triton–milk–PBS-T was used as the dilution buffer for the samples. After being washed three times with PBS-T, anti-GST-EBO-R-ΔNP rabbit serum and anti-His-EBO-Z-rNP rabbit serum at a dilution of 1:1,000 were added to the wells of the plates coated with the Res2-6C8 or Res2-1D8 and 3-3D, respectively. The plates were incubated for 1 h at 37°C and washed three times with PBS-T. Then, horseradish peroxidase-conjugated goat anti-rabbit IgG (H+L) antiserum (catalog no. 62-6120; Zymed Laboratories, Inc.) was added to the wells at a dilution of 1:1,000, and the plates were incubated for 1 h at 37°C. After being washed three times with PBS-T, 2,2′-azinobis[3-ethylbenziazoline-6-sulfonic acid] (ABTS) substrate (ABTS tablet and buffer; Roche Diagnostics, Mannheim, Germany) was added to the wells. The plates were then incubated for 30 min at room temperature, and the optical density at 405 nm (OD) was recorded.

In the antigen capture ELISAs using Res2-6C8, Res2-1D8, and 3-3D, the mean + 3 standard deviations (SDs) of OD of 79 sera from EBO-R-uninfected macaques were 0.11, 0.07, and 0.11, respectively, and those of 5 livers from EBO-R-uninfected macaques were 0.15, 0.08, and 0.15, respectively. Therefore, we defined the cutoff value as 0.2 in the assay.

RESULTS

Development of two MAbs specific to the EBO-R NP. Thirty-two hybridoma clones secreting MAbs to EBO-R rNP were established, and the reactivities of these MAbs to His-EBO-R-NP were examined in the antigen capture ELISA format

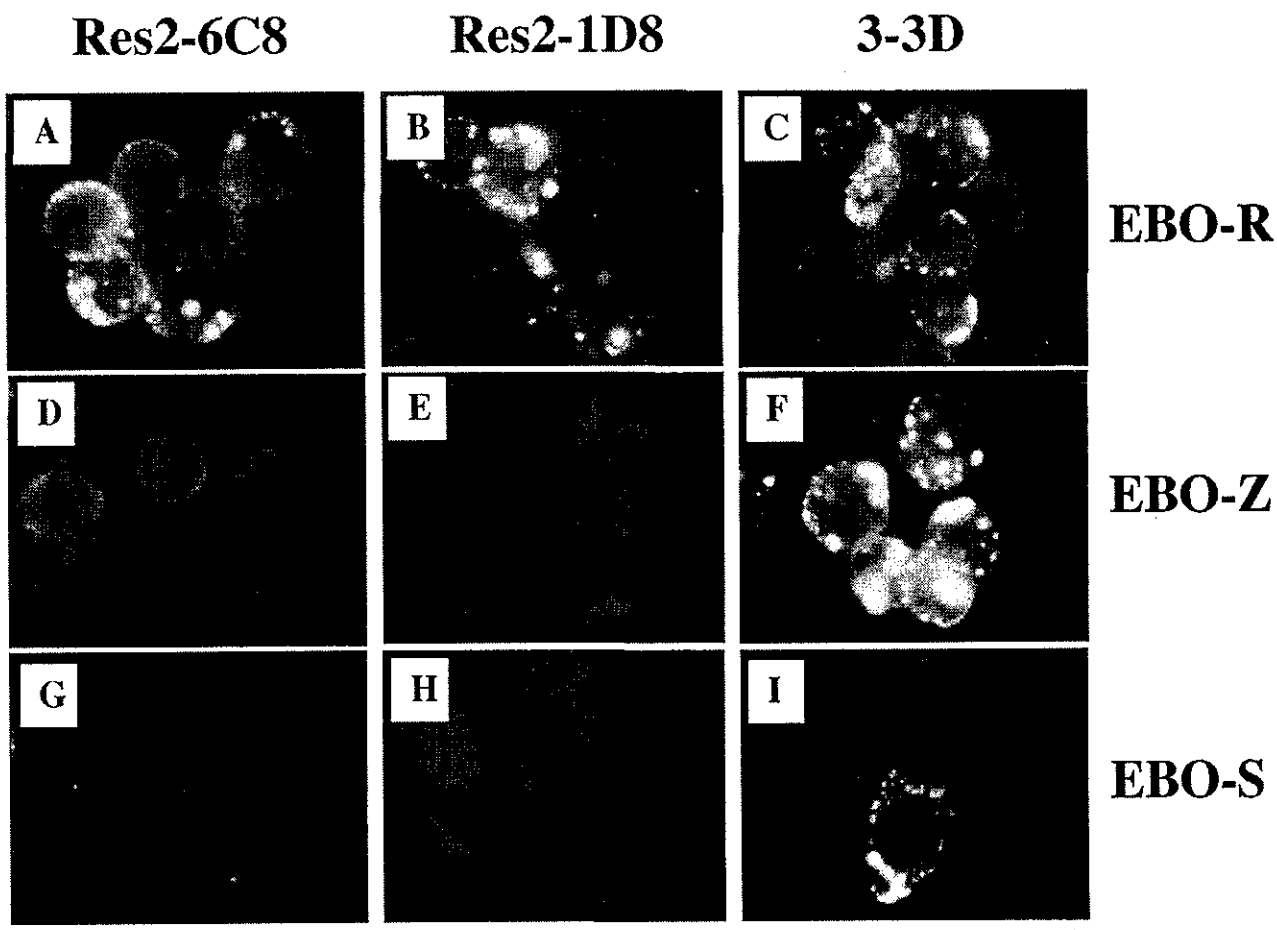

FIG. 1. IFA using HeLa cells expressing rNP of EBO-R (A to C) or EBO-Z (D-F) and using Vero cells infected with EBO-S (G to I). The reactivities of Res2-6C8 (A, D, and G), Res2-1D8 (B, E, and H), and 3-3D (C, F, and I) to NP of EBO-R, EBO-Z, and EBO-S are shown. Res2-6C8 and Res2-1D8 reacted to EBO-R NP, but not to the NPs of EBO-Z and EBO-S. The MAb 3-3D reacts to the NPs of all three Ebola virus species.

(data not shown). Two MAbs, Res2-6C8 and Res2-1D8, were reactive in the antigen capture ELISA format and were used in the present study. The isotypes of Res2-6C8 and Res2-1D8 were IgG2b and IgG1, respectively. Ebola virus species specificity of Res2-6C8 and Res2-1D8 was examined by IFA with HeLa cells that expressed the rNP of EBO-R or EBO-Z or by using Vero E6 cells infected with EBO-S. These two MAbs reacted to EBO-R NP (Fig. 1A and B), but not to EBO-Z NP (Fig. 1D and E) or EBO-S NP (Fig. 1G and H).

Epitopes recognized by Res2-6C8 and Res2-1D8. The epitopes recognized by Res2-6C8 and Res2-1D8 were determined by IgG ELISAs using the truncated EBO-R rNPs (Fig. 2). Res2-6C8 and Res2-1D8 recognized the amino acid residues between aa 631 and 739, and the minimum epitopes were further determined. Res2-6C8 reacted to the truncated EBO-R rNPs corresponding to aa 636 to 739 and 631 to 639, but not to aa 637 to 739 and 631 to 638. On the other hand, Res2-1D8 reacted to the truncated EBO-R NP corresponding to aa 636 to 739 and 631 to 643, but not to aa 637 to 739 and 631 to 642. These results showed that the epitopes recognized by Res2-6C8 and Res2-1D8 were aa 636 to 639 (4 aa residues, $_{636}$DPDI$_{639}$) and aa 636 to 643 (8 aa residues, $_{636}$DPDIGQSK$_{643}$) of EBO-R NP, respectively. The amino acid sequences of the epitopes were aligned to that of EBO-R Pennsylvania isolate in 1989 to 1990, EBO-Z, and EBO-S. The 8 aa residues were identical to those of the EBO-R Pennsylvania isolate in 1989 to 1990 (Table 2). The amino acid sequences of EBO-Z and EBO-S NPs corresponding to the amino acids of EBO-R, $_{636}$DPDIGQSK$_{643}$, were NQDSDNTQ and EALPINSK, respectively (Table 2).

Development of the antigen capture ELISAs using these novel MAbs. The sensitivity of the antigen capture ELISAs prepared with these two MAbs was tested. As shown in Fig. 3A, Res2-6C8 and Res2-1D8 detected His-EBO-R-NP up to dilutions of 1:128,000 and 1:64,000 in the antigen capture ELISA, respectively. The ELISA prepared with 3-3D detected His-EBO-R-NP up to the dilution of 1:32,000. As expected, Res2-6C8 and Res2-1D8 did not detect His-EBO-Z-NP in the antigen capture ELISA (Fig. 3B).

Detection of EBO-R NP in the specimens from EBO-R-infected monkeys. Serum, liver, and spleen specimens from EBO-R-infected macaques were examined for the presence of EBO-R NP by antigen capture ELISAs using Res2-6C8, Res2-1D8, and 3-3D. Res2-6C8 and Res2-1D8 detected the EBO-R NP antigens in the sera, livers, and spleens (Table 3). Res2-6C8 detected the NP in all of the samples, while Res2-1D8 and 3-3D detected the NP in six of seven and five of seven samples,

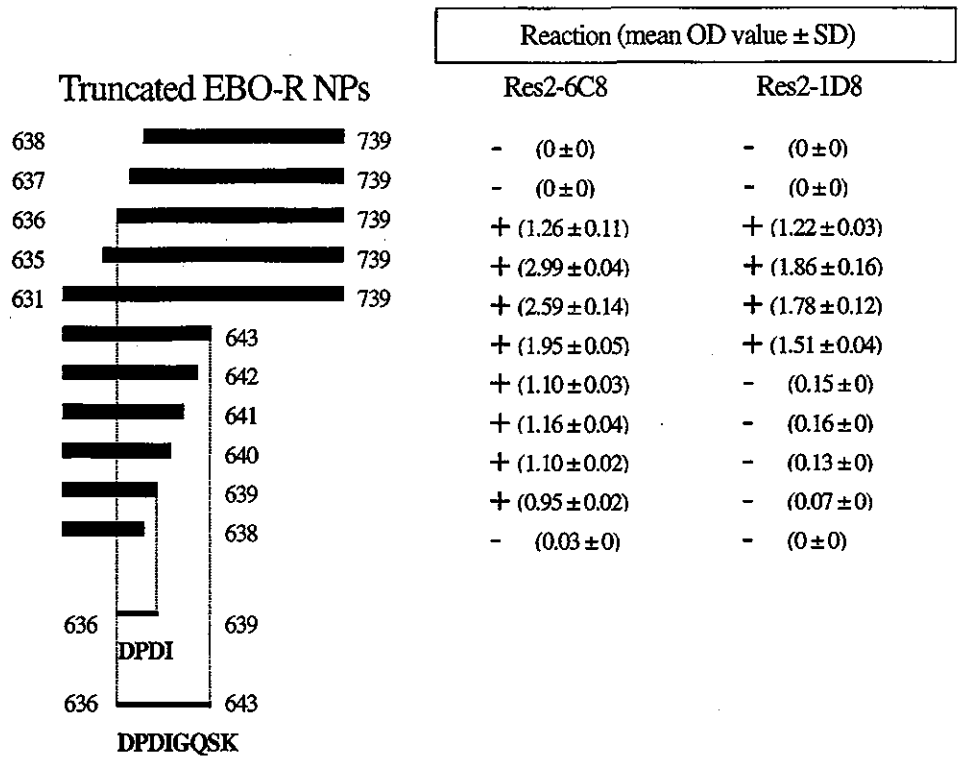

FIG. 2. Reactivities of Res2-6C8 and Res2-1D8 to the truncated EBO-R rNPs in IgG ELISA. Res2-6C8 recognizes the amino acid residues between aa 636 and 639 (sequence, DPDI). Res2-1D8 recognizes the amino acid residues between aa 636 and 643 (sequence, DPDIGQSK). The mean OD value ± SD in the IgG ELISA is shown.

respectively. The endpoint titers were higher in the ELISAs using Res2-6C8 and Res2-1D8 than in the ELISA using 3-3D.

DISCUSSION

We previously established an antigen capture ELISA using the MAb 3-3D, which reacted to the NPs of EBO-Z, EBO-S, and EBO-R (29). The minimum epitope recognized by MAb 3-3D was mapped on 26 aa residues between aa 648 and 673 at the C-terminal region of the EBO-Z NP (29), and the amino acid residues between aa 631 and 739 and aa 633 and 738 were required for the cross-reaction to EBO-R NP and EBO-S NP, respectively (29). In the present study, we developed two novel MAbs to EBO-R NP, Res2-6C8 and Res2-1D8, which detected EBO-R NP with high sensitivity and specificity in the antigen capture ELISA format. The minimum epitopes recognized by Res2-6C8 and Res2-1D8 were found to be $_{636}$DPDI$_{639}$ and $_{636}$DPDIGQSK$_{643}$, respectively (Fig. 2). The amino acid se-

TABLE 2. Comparison of the epitopes of Res2-6C8 and Res2-1D8

Ebola virus species[a]	Amino acids corresponding to epitope of:	
	Res2-6C8	Res2-1D8
EBO-R, 1996	$_{636}$DPDI$_{639}$	$_{636}$DPDIGQSK$_{643}$
EBO-R, 1989/1990	$_{636}$DPDI$_{639}$	$_{636}$DPDIGQSK$_{643}$
EBO-Z, 1976	$_{636}$NQDS$_{639}$	$_{636}$NQDSDNTQ$_{643}$
EBO-S, 1976	$_{636}$EALP$_{639}$	$_{636}$EALPINSK$_{643}$

[a] GenBank accession no.: EBO-R, 1996, AB050936; EBO-R, 1989/1990, AF522874; EBO-Z, 1976, AF086833; and EBO-S, 1976, AF173836.

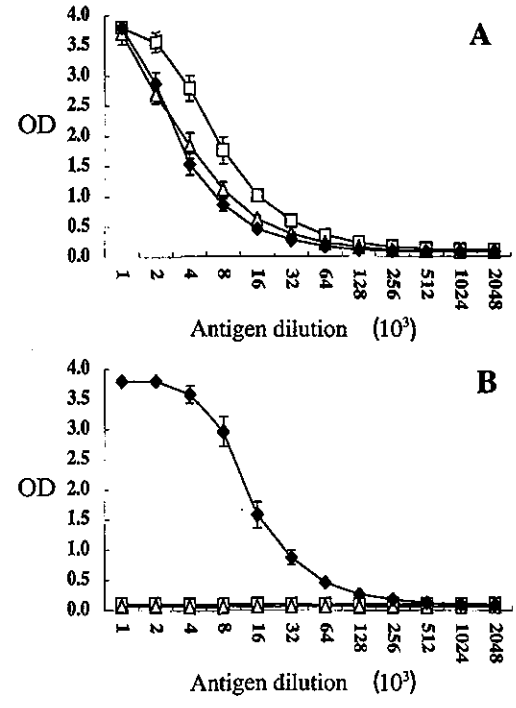

FIG. 3. Reactivity of MAbs Res2-6C8 (□), Res2-1D8 (△), and 3-3D (◆) to the rNPs of EBO-R and EBO-Z in the antigen capture ELISA. His-EBO-R-NP (A) and His-EBO-Z-NP (B) were used as antigens. The mean ± SD of four assays is shown.

TABLE 3. Detection of EBO-R NP from clinical specimens

Sample	Monkey no.	Titer by antigen capture ELISA[a]			Result by:	
		Res2-6C8	Res2-1D8	3-3D[b]	RT-PCR[c]	IHC[d]
Serum	2612	160	40	20	+	+
	2866	320	320	160	+	ND
Liver	2877	40	<10	10	ND[e]	ND
	2882	160	40	40	+	+
Spleen	2877	320	160	80	ND	ND
	2882	80	20	<10	ND	+
	2885	160	40	<10	+	ND

[a] Antigen titer in the specimens. The antigen titer in the ELISA was determined as the reciprocal of the highest dilution showing a positive reaction. The titer was determined by a single test. The cutoff OD value was 0.2.
[b] Ebola virus species cross-reactive MAb (29).
[c] RT-PCR with primers RES-Nf2 and RES-Nr2.
[d] IHC, immunohistochemistry for the detection of Ebola virus NP (14).
[e] ND, not done.

quence of EBO-R NP, $_{636}$DPDIGQSK$_{643}$, was different from those of EBO-Z and EBO-S NP (Table 2). This is consistent with the result in which the two MAbs did not react to the NP of EBO-Z and EBO-S in the IFA (Fig. 1D, E, G, and H). The amino acid sequences of the epitopes recognized by the two MAbs were identical to those of EBO-R Pennsylvania isolate in 1989 to 1990 (Table 2) (11, 13). Considering the genetic stability among EBO-R isolates (11, 13), it is expected that antigen capture ELISA systems using Res2-6C8 and Res2-1D8 detect either EBO-R strain.

We determined the cutoff value in the antigen capture ELISA based on the mean OD value + 3 SDs of 79 sera and 5 liver specimens from EBO-R-uninfected cynomolgus macaques. Since the mean OD value + 3 SDs was lower than 0.2 in any specimen, the cutoff value was determined to be 0.2 in the present study. The sensitivity of the antigen capture ELISA using either Res2-6C8 or Res2-1D8 for His-EBO-R-NP was similar to that using 3-3D (Fig. 3A). On the other hand, His-EBO-Z-NP was not detected in the antigen capture ELISAs using Res2-6C8 and Res2-1D8 (Fig. 3B), as expected from the results in the IFA and the epitope sequences, demonstrating that the antigen capture ELISAs using Res2-6C8 and Res2-1D8 were specific to EBO-R.

Authentic EBO-R NP in the serum, liver, and spleen specimens from the macaques naturally infected with EBO-R was detected by the antigen capture ELISAs using the Res2-6C8, Res2-1D8, and 3-3D MAbs (Table 3). The sensitivity of the ELISA in detecting the authentic EBO-R NP was higher with Res2-6C8 and Res2-1D8 than with 3-3D. Since the clinical specimens used in this study were stored for 6 years, it is possible that the EBO-R NP was somewhat degraded and was detected with higher sensitivity by Res2-6C8, which recognizes 4 aa of the NP, than by 3-3D, which recognizes 109 aa. The results, nevertheless, indicated that both Res2-6C8 and Res2-1D8 were highly sensitive in detecting EBO-R NP in clinical specimens.

An outbreak of EBO-CI occurred among a troop of chimpanzees in the Taï National Park, Ivory Coast, in 1994 (20). It was also reported that Ebola hemorrhagic fever patients had been infected with Ebola virus while butchering dead chimpanzees in the first outbreak in Gabon during 1996 (1, 8, 9). Fatal infection with EBO-Z, EBO-S, EBO-CI, and EBO-R was also demonstrated in cynomolgus macaques (7). EBO-R caused outbreaks among cynomolgus macaques in the Philippines (2–4, 12, 16, 25, 30, 38) and is most likely to cause epizootics among Asian macaques. Since EBO-R has never caused symptomatic infection in humans (3, 4, 25, 38), rapid differentiation of the species of Ebola virus is crucial, especially when samples from nonhuman primates are tested. Although RT-PCR has higher sensitivity to Ebola virus than the antigen capture ELISA, the sequencing of the PCR products is essential for confirming Ebola virus infection (21–23, 30, 34, 35). The viral load in the blood and other organs has been shown to reach extremely high levels in Ebola virus-infected animals (5, 7, 17, 31). Thus, the newly developed antigen capture ELISAs using Res2-6C8 and Res2-1D8 might be a promising tool for the diagnosis of EBO-R infection, especially in monkey quarantine and field studies.

ACKNOWLEDGMENTS

We gratefully acknowledge M. Ogata of the National Institute of Infectious Diseases and the staff of the Research Institute for Tropical Medicine for technical assistance.

This work was partly supported by a grant from the Ministry of Health, Labour, and Welfare, Japan.

REFERENCES

1. **Baize, S., E. M. Leroy, M. C. Georges-Courbot, M. Capron, J. Lansoud-Soukate, P. Debre, S. P. Fisher-Hoch, J. B. McCormick, and A. J. Georges.** 1999. Defective humoral responses and extensive intravascular apoptosis are associated with fatal outcome in Ebola virus-infected patients. Nat. Med. 5:423–426.
2. **Centers for Disease Control and Prevention.** 1996. Ebola-Reston virus infection among quarantined nonhuman primates—Texas, 1996. Morb. Mortal. Wkly. Rep. 45:314–316.
3. **Centers for Disease Control and Prevention.** *1990. Epidemiologic notes and* reports updates: filovirus infection in animal handlers. Morb. Mortal. Wkly. Rep. 39:221.
4. **Centers for Disease Control and Prevention.** 1990. Update: filovirus infections among persons with occupational exposure to nonhuman primates. Morb. Mortal. Wkly. Rep. 39:266–273.
5. **Connolly, B. M., K. E. Steele, K. J. Davis, T. W. Geisbert, W. M. Kell, N. K. Jaax, and P. B. Jahrling.** 1999. Pathogenesis of experimental Ebola virus infection in guinea pigs. J. Infect. Dis. 179(Suppl. 1):S203–S217.
6. **Feldmann, H., H. D. Klenk, and A. Sanchez.** 1993. Molecular biology and evolution of filoviruses. Arch. Virol. 7(Suppl.):S81–S100.
7. **Fisher-Hoch, S. P., T. L. Brammer, S. G. Trappier, L. C. Hutwagner, B. B. Farrar, S. L. Ruo, B. G. Brown, L. M. Hermann, G. I. Perez-Oronoz, C. S. Goldsmith, M. A. Hanes, and J. B. McCormick.** 1992. Pathogenic potential of filoviruses: role of geographic origin of primate host and virus strain. J. Infect. Dis. 166:753–763.
8. **Georges, A. J., E. M. Leroy, A. A. Renaut, C. T. Benissan, R. J. Nabias, M. T. Ngoc, P. I. Obiang, J. P. Lepage, E. J. Bertherat, D. D. Benoni, E. J. Wickings, J. P. Amblard, J. M. Lansoud-Soukate, J. M. Milleliri, S. Baize, and M. C. Georges-Courbot.** 1999. Ebola hemorrhagic fever outbreaks in Gabon, 1994–1997: epidemiologic and health control issues. J. Infect. Dis. 179(Suppl. 1):S65–S75.
9. **Georges-Courbot, M. C., A. Sanchez, C. Y. Lu, S. Baize, E. Leroy, J. Lansout-Soukate, C. Tevi-Benissan, A. J. Georges, S. G. Trappier, S. R. Zaki, R. Swanepoel, P. A. Leman, P. E. Rollin, C. J. Peters, S. T. Nichol, and T. G. Ksiazek.** 1997. Isolation and phylogenetic characterization of Ebola viruses causing different outbreaks in Gabon. Emerg. Infect. Dis. 3:59–62.
10. **Gibb, T. R., D. A. Norwood, Jr., N. Woollen, and E. A. Henchal.** 2001. Development and evaluation of a fluorogenic 5′ nuclease assay to detect and differentiate between Ebola virus subtypes Zaire and Sudan. J. Clin. Microbiol. 39:4125–4130.
11. **Groseth, A., U. Stroher, S. Theriault, and H. Feldmann.** 2002. Molecular characterization of an isolate from the 1989/90 epizootic of Ebola virus Reston among macaques imported into the United States. Virus Res. 87:155.
12. **Hayes, C. G., J. P. Burans, T. G. Ksiazek, R. A. Del Rosario, M. E. Miranda, C. R. Manaloto, A. B. Barrientos, C. G. Robles, M. M. Dayrit, and C. J. Peters.** 1992. Outbreak of fatal illness among captive macaques in the Philippines caused by an Ebola-related filovirus. Am. J. Trop. Med. Hyg. 46: 664–671.

13. **Ikegami, T., A. B. Calaor, M. E. Miranda, M. Niikura, M. Saijo, I. Kurane, Y. Yoshikawa, and S. Morikawa.** 2001. Genome structure of Ebola virus subtype Reston: differences among Ebola subtypes. Arch. Virol. **146**:2021–2027.
14. **Ikegami, T., M. E. Miranda, A. B. Calaor, D. L. Manalo, N. J. Miranda, M. Niikura, M. Saijo, Y. Une, Y. Nomura, I. Kurane, T. G. Ksiazek, Y. Yoshikawa, and S. Morikawa.** 2002. Histopathology of natural Ebola virus subtype Reston infection in cynomolgus macaques during the Philippine outbreak in 1996. Exp. Anim. **51**:447–455.
15. **Ikegami, T., M. Saijo, M. Niikura, M. E. Miranda, A. B. Calaor, M. Hernandez, D. L. Manalo, I. Kurane, Y. Yoshikawa, and S. Morikawa.** 2002. Development of an immunofluorescence method for the detection of antibodies to Ebola virus subtype Reston by the use of recombinant nucleoprotein-expressing HeLa cells. Microbiol. Immunol. **46**:633–638.
16. **Jahrling, P. B., T. W. Geisbert, D. W. Dalgard, E. D. Johnson, T. G. Ksiazek, W. C. Hall, and C. J. Peters.** 1990. Preliminary report: isolation of Ebola virus from monkeys imported to USA. Lancet **335**:502–505.
17. **Jahrling, P. B., T. W. Geisbert, N. K. Jaax, M. A. Hanes, T. G. Ksiazek, and C. J. Peters.** 1996. Experimental infection of cynomolgus macaques with Ebola-Reston filoviruses from the 1989–1990 U.S. epizootic. Arch. Virol. **11**(Suppl.):S115–S134.
18. **Ksiazek, T. G., P. E. Rollin, P. B. Jahrling, E. Johnson, D. W. Dalgard, and C. J. Peters.** 1992. Enzyme immunosorbent assay for Ebola virus antigens in tissues of infected primates. J. Clin. Microbiol. **30**:947–950.
19. **Ksiazek, T. G., P. E. Rollin, A. J. Williams, D. S. Bressler, M. L. Martin, R. Swanepoel, F. J. Burt, P. A. Leman, A. S. Khan, A. K. Rowe, R. Mukunu, A. Sanchez, and C. J. Peters.** 1999. Clinical virology of Ebola hemorrhagic fever (EHF): virus, virus antigen, and IgG and IgM antibody findings among EHF patients in Kikwit, Democratic Republic of the Congo, 1995. J. Infect. Dis. **179**(Suppl. 1):S177–S187.
20. **Le Guenno, B., P. Formentry, M. Wyers, P. Gounon, F. Walker, and C. Boesch.** 1995. Isolation and partial characterization of a new strain of Ebola virus. Lancet **345**:1271–1274.
21. **Leroy, E. M., S. Baize, C. Y. Lu, J. B. McCormick, A. J. Georges, M. C. Georges-Courbot, J. Lansoud-Soukate, and S. P. Fisher-Hoch.** 2000. Diagnosis of Ebola haemorrhagic fever by RT-PCR in an epidemic setting. J. Med. Virol. **60**:463–467.
22. **Leroy, E. M., S. Baize, V. E. Volchkov, S. P. Fisher-Hoch, M. C. Georges-Courbot, J. Lansoud-Soukate, M. Capron, P. Debre, J. B. McCormick, and A. J. Georges.** 2000. Human asymptomatic Ebola infection and strong inflammatory response. Lancet **355**:2210–2215.
23. **Lloyd, E. S., S. R. Zaki, P. E. Rollin, K. Tshioko, M. A. Bwaka, T. G. Ksiazek, P. Calain, W. J. Shieh, M. K. Konde, E. Verchueren, H. N. Perry, L. Manguindula, J. Kabwau, R. Ndambi, and C. J. Peters.** 1999. Long-term disease surveillance in Bandundu region, Democratic Republic of the Congo: a model for early detection and prevention of Ebola hemorrhagic fever. J. Infect. Dis. **179**(Suppl. 1):S274–S280.
24. **Matsuura, Y., R. D. Possee, H. A. Overton, and D. H. Bishop.** 1987. Baculovirus expression vectors: the requirements for high level expression of proteins, including glycoproteins. J. Gen. Virol. **68**:1233–1250.
25. **Miranda, M. E., T. G. Ksiazek, T. J. Retuya, A. S. Khan, A. Sanchez, C. F. Fulhorst, P. E. Rollin, A. B. Calaor, D. L. Manalo, M. C. Roces, M. M. Dayrit, and C. J. Peters.** 1999. Epidemiology of Ebola (subtype Reston) virus in the Philippines, 1996. J. Infect. Dis.**179**(Suppl. 1):S115–S119.
26. **Mühlberger, E., M. Weik, V. E. Volchkov, H. D. Klenk, and S. Becker.** 1999. Comparison of the transcription and replication strategies of Marburg virus and Ebola virus by using artificial replication systems. J. Virol. **73**:2333–2342.
27. **Netesov, S. V., H. Feldmann, P. B. Jahrling, H.-D. Klenk, and A. Sanchez.** 2002. Family *Filoviridae*, p. 539–548. *In* M. H. V. van Regenmortel, C. M. Fauquet, D. H. L. Bishop, E. B. Carstens, M. K. Estes, S. M. Lemon, J. Maniloff, M. A. Mayo, D. J. McGeoch, C. R. Pringle, and R. B. Wickner (ed.), Virus taxonomy. The Seventh Report of the International Committee on Taxonomy of Viruses. Academic Press, San Diego, Calif.
28. **Niikura, M., T. Ikegami, M. Saijo, T. Kurata, I. Kurane, and S. Morikawa.** 2003. Analysis of linear B-cell epitopes of the nucleoprotein of Ebola virus that distinguish Ebola virus subtypes. Clin. Diagn. Lab. Immunol. **10**:83–87.
29. **Niikura, M., T. Ikegami, M. Saijo, I. Kurane, M. E. Miranda, and S. Morikawa.** 2001. Detection of Ebola viral antigen by enzyme-linked immunosorbent assay using a novel monoclonal antibody to nucleoprotein. J. Clin. Microbiol. **39**:3267–3271.
30. **Rollin, P. E., R. J. Williams, D. S. Bressler, S. Pearson, M. Cottingham, G. Pucak, A. Sanchez, S. G. Trappier, R. L. Peters, P. W. Greer, S. Zaki, T. Demarcus, K. Hendricks, M. Kelley, D. Simpson, T. W. Geisbert, P. B. Jahrling, C. J. Peters, and T. G. Ksiazek.** 1999. Ebola (subtype Reston) virus among quarantined nonhuman primates recently imported from the Philippines to United States. J. Infect. Dis. **179**(Suppl. 1):S108–S114.
31. **Ryabchikova, E. I., L. V. Kolesnikova, and S. V. Luchko.** 1999. An analysis of features of pathogenesis in two animal models of Ebola virus infection. J. Infect. Dis. **179**(Suppl. 1):S199–S202.
32. **Saijo, M., M. Niikura, S. Morikawa, and I. Kurane.** 2001. Immunofluorescence method for detection of Ebola virus immunoglobulin G, using HeLa cells which express recombinant nucleoprotein. J. Clin. Microbiol. **39**:776–778.
33. **Saijo, M., M. Niikura, S. Morikawa, T. G. Ksiazek, R. F. Meyer, C. J. Peters, and I. Kurane.** 2001. Enzyme-linked immunosorbent assays for detection of antibodies to Ebola and Marburg viruses using recombinant nucleoproteins. J. Clin. Microbiol. **39**:1–7.
34. **Sanchez, A., A. S. Khan, S. R. Zaki, G. J. Nabel, T. G. Ksiazek, and C. J. Peters.** 2001. *Filoviridae*: Marburg and Ebola viruses. p. 1279–1304. *In* D. M. Knipe and P. M. Howley (ed.), Fields virology, 4th ed. Lippincott, Williams & Wilkins, Philadelphia, Pa.
35. **Sanchez, A., T. G. Ksiazek, P. E. Rollin, M. E. Miranda, S. G. Trappier, A. S. Khan, C. J. Peters, and S. T. Nichol.** 1999. Detection and molecular characterization of Ebola viruses causing disease in human and nonhuman primates. J. Infect. Dis. **179**(Suppl. 1):S164–S169.
36. **World Health Organization.** 1976. Ebola haemorrhagic fever in Sudan, 1976. Bull. W. H. O. **56**:247–270.
37. **World Health Organization.** 1978. Ebola haemorrhagic fever in Zaire, 1976. Report of an international commission. Bull. W. H. O. **56**:271–293.
38. **World Health Organization.** 1992. Viral haemorrhagic fever in imported monkeys. Wkly. Epidemiol. Rec. **67**:142–143.
39. **Zaki, S. R., W. J. Shieh, P. W. Greer, C. S. Goldsmith, T. Ferebee, J. Katshitshi, F. K. Tshioko, M. A. Bwaka, R. Swanepoel, P. Calain, A. S. Khan, E. Lloyd, P. E. Rollin, T. G. Ksiazek, and C. J. Peters.** 1999. A novel immunohistochemical assay for the detection of Ebola virus in skin: implications for diagnosis, spread, and surveillance of Ebola hemorrhagic fever. J. Infect. Dis. **179**(Suppl. 1):S36–S47.

Virology 305, 288–297 (2003)
doi:10.1006/viro.2002.1767

The Intracellular Association of the Nucleocapsid Protein (NP) of Hantaan Virus (HTNV) with Small Ubiquitin-like Modifier-1 (SUMO-1) Conjugating Enzyme 9 (Ubc9)

Akihiko Maeda,* Byoung-Hee Lee,† Kumiko Yoshimatsu,† Masayuki Saijo,* Ichiro Kurane,* Jiro Arikawa,† and Shigeru Morikawa*,[1]

*Department of Virology 1, National Institute of Infectious Diseases, Musashimurayama, Tokyo, Japan; and †Institute of Animal Experimentation, School of Medicine, Hokkaido University, Sapporo, Japan

Received June 14, 2002; returned to author for revision July 29, 2002; accepted September 6, 2002

Small ubiquitin-like modifier-1 (SUMO-1) conjugating enzyme 9 (Ubc9) conjugates SUMO-1 to target proteins and modulates cellular processes such as signal transduction, transcription regulation, and cell growth regulation. We demonstrated here that the nucleocapsid protein (NP) of Hantaan virus (HTNV) was associated with Ubc9 and SUMO-1 *in vivo*. Analysis of the interaction between the truncated NPs and Ubc9 revealed that the amino acid residues at the positions between 101 and 238 in the NP were responsible for the interaction. Furthermore, a consensus binding motif of Ubc9 and SUMO-1, MKAE, within this region, especially the second amino acid of the motif, K residue, was crucial for the interaction, and the interaction was essential for the NP to be localized in the perinuclear region. These results indicate that the assembly of the HTNV-NP is regulated by the interaction between the NP and Ubc9. This is the first report to demonstrate the interaction of Ubc9 with a structural protein of negative-strand RNA viruses.

Key Words: HTNV; NP; Ubc9; SUMO-1; localization of the NP

INTRODUCTION

Hantaviruses are associated with two severe diseases in humans; hemorrhagic fever with renal syndrome (HFRS) and hantavirus pulmonary syndrome (HPS) (*7, 8, 21*). Hantaan virus (HTNV) belongs to the genus Hantavirus, the family *Bunyaviridae* (*29*), and is an enveloped virus with a diameter of 120 nm possessing tripartite-segmented, single-stranded, negative sense RNA genomes (*40*). The small (S)-RNA encodes a viral nucleocapsid protein (NP) (*41*), The middle (M)-RNA encodes two glycoproteins (G1 and G2) (*42*), and the large (L)-RNA encodes an RNA-dependent RNA polymerase (*39*).

The NP of hantavirus, a protein with a molecular weight of approximately 50 kDa, makes a viral ribonucleocapsid (RNP) complex and directs viral RNA synthesis. The NP localizes at the perinuclear region in infected or NP-expressing cells (*31*). The NP of hantavirus has been shown to form a multimer both *in vivo* and *in vitro* (*2*) and its carboxyl (C)-terminal half and amino (N)-terminal 40-amino acid (aa) residues are responsible for the oligomerization of the NP (Fig. 1) (*2*). The N-terminal 40-aa residues, in particular, may form trimeric coiled-coils and contribute to NP trimerization. The NP-trimers are thought to be intermediates in the assembly of the RNP of hantavirus. After the formation of the NP-trimers and viral genomic RNA complexes, the NP-trimers gradually assemble into long multimers together with the RNAs. In addition, the viral RNAs bind directly to the NP *in vivo* and *in vitro* (*12, 17, 30, 35, 44, 45*). Even though a great deal of experimental data containing viral replication and assembly has been recently reported, it is still unclear how the virus assembles itself from the various constituent viral structural proteins and viral genomic RNAs, and what kinds of host proteins are involved in the viral assembly or replication.

To address the host factors involved in the assembly of the RNP and replication of HTNV, it is crucial to define the cellular proteins interacting with the NP. In this study, we focused on small ubiquitin-like modifier-1 (SUMO-1) conjugating enzyme 9 (Ubc9) (*27*), which strongly interacts with the NP in a yeast two-hybrid system. We showed that Ubc9 interacted with the HTNV-NP and identified the region within the HTNV-NP responsible for binding to Ubc9. Furthermore, our present data indicated that the interaction of the NP with Ubc9 determined the localization of the NP at the perinuclear region where viral replication and assembly should occur.

RESULTS

Interaction between the NP and the Ubc9 in yeast cells

In many viruses, the NPs play crucial roles in viral RNP assembly and replication (*19, 20, 22*). It might also be possible that some cellular proteins are involved in these

[1] To whom correspondence and reprint requests should be addressed at 4-7-1 Gakuen, Musashimurayama, Tokyo 208-0011, Japan. Fax: +81-42-564-4881. Email: morikawa@nih.go.jp.

0042-6822/03 $30.00

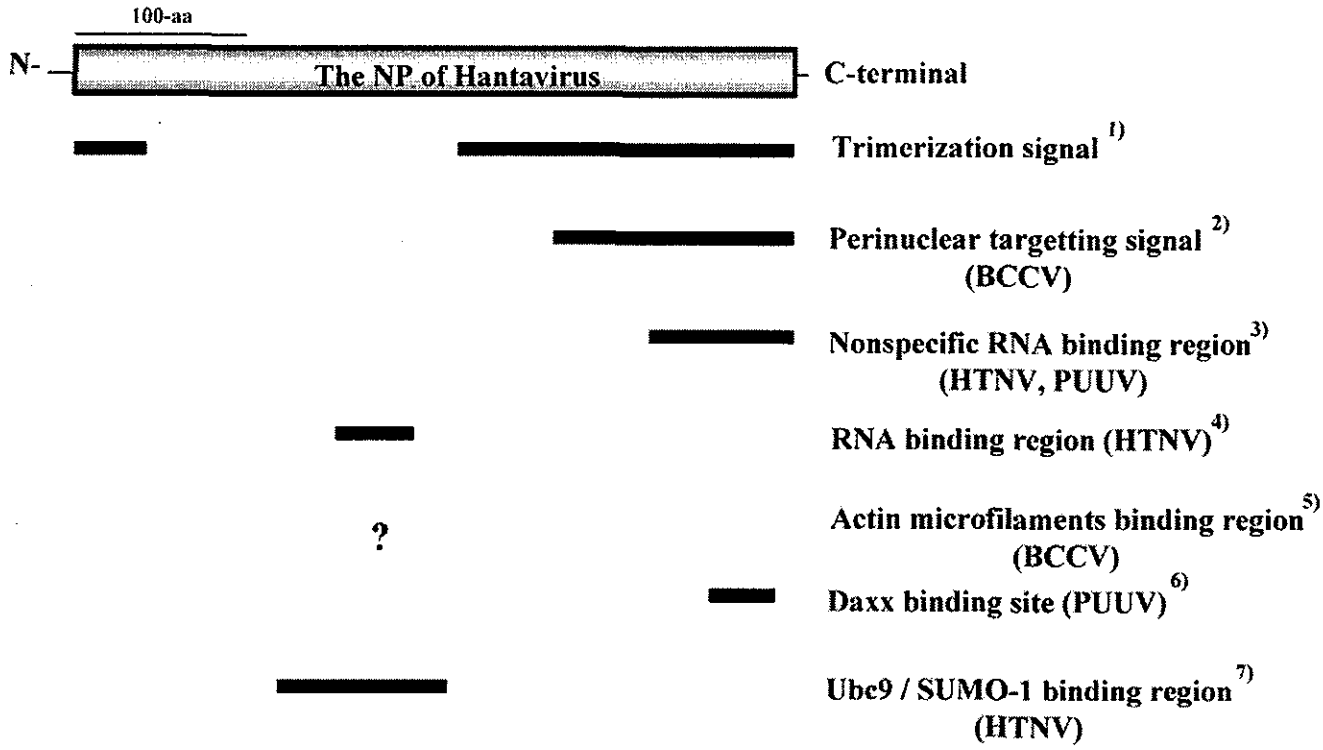

FIG. 1. A schematic representation of the functional domains in the NP of hantaviruses. According to published reports, the functional domains (shown as black bars) in the NP are as followes: 1) the NP trimerization signal (Alfadhli, *et al.*, 2001) (2), 2) the perinuclear targeting signal (Ravkov, *et al.*, 2001) (31), 3) the nonspecific RNA binding region (Gott, *et al.*, 1993) (12), 4) the specific RNA binding region (Xu, *et al.*, 2002) (50), 6) the actin microfilament binding region (Ravkov, *et al.*, 1998) (32), 6) the Daxx binding site (Li *et al.*, 2002) (23), and 7) the Ubc9/SUMO-1 binding region (in this study).

events. Such cellular proteins should function through the interaction with the NP. We have employed a yeast two-hybrid system to define the cellular proteins that interact with the NP of HTNV, using the cDNA library derived from HeLa cells as a target. From 1×10^6 independent cDNA clones, we obtained 11 cDNA clones that strongly interacted with the HTNV-NP in yeast cells. The nucleotide sequences of 2 of these 11 clones were identical to that of Ubc9 (*49*) (data not shown). We measured β-Gal activity in the yeast cells cotransformed with the bait-NP protein expression vector, pAS2–1-HTN-NP, and the prey-*Ubc9 protein* expression vector, pACT2-Ubc9. β-Galactosidase (β-Gal) activity in the yeast cells transformed with both vectors was around 3400 times higher than those in the yeast cells transformed with pAS2–1-HTN-NP and pACT2 or pAS2–1 and pACT2-Ubc9, and around 30 times higher than that in pAS2–1 and pACT2. This result indicates that the HTNV-NP interacted with Ubc9 in the yeast cells.

Interaction between the NP and Ubc9 in mammalian cells

We also examined the interaction between the NP of HTNV and the Ubc9 in mammalian cells. We transfected 293T cells with vectors for a mammalian *two-hybrid system*, pBIND-HTNV-NP and pACT-Ubc9, and with pG5*luc*. The luciferase activity in 293T cells transfected with pBIND-HTN-NP and pACT-Ubc9 was higher than that in the 293T cells transfected with pBIND-HTN-NP and pACT, pBIND and pACT-Ubc9, or pBIND and pACT (Fig. 2A). Similar results were obtained in the experiment using Vero E6 cells (data not shown). The results strongly suggest that the HTNV-NP actually interacted with Ubc9 in mammalian cells.

To examine the subcellular localization of the NP and Ubc9 in mammalian cells, enhanced green fluorescent protein (EGFP)-tagged Ubc9 was transiently expressed in HTNV-infected Vero E6 cells by transfection with pEGFP-C1-Ubc9. *As shown* in Fig. 2B, EGFP-tagged Ubc9 was mainly localized in the perinuclear region and was colocalized with the NP of HTNV. The EGFP-tagged Ubc9 and the NP were also colocalized in the cytoplasm when these two proteins were both transiently expressed using the expression vectors (data not shown).

Mapping of the Ubc9-binding region within the NP of HTNV

To determine the Ubc9-binding region within the NP, we first introduced a series of deletions into the NP gene of the yeast vector, pAS2-1-HTN-NP (Fig. 3), and cotransformed Y190 yeast cells with the pAS2-1-HTN-NP containing the deletions in the *HTN-NP and* pACT2-

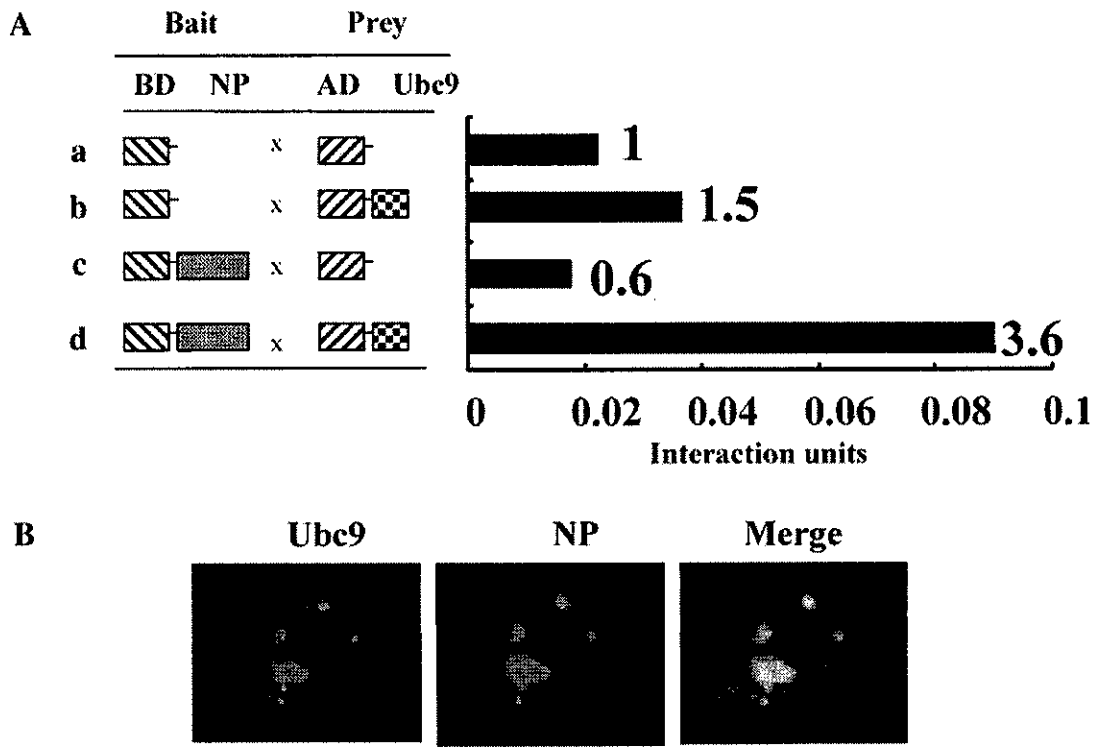

FIG. 2. Interaction between the NP of HTNV and Ubc9 in the mammalian cells. (A) Mammalian two-hybrid assay for examining the interaction between the NP and Ubc9 in 293T cells. Mammalian two-hybrid vectors, pBIND vector and pACT vector, were cotransfected with pG5 *luc* into 293T cells (a). pBIND and pACT-Ubc9 (b), pBIND-HTN-NP and pACT (c), and pBIND-HTN-NP and pACT Ubc9 (d) were also cotransfected with pG5 *luc*. Luciferase activities were measured at 48 h.p.t. as described in the text. The bait domain (BD), the NP, the prey domain (AD) and Ubc9 are illustrated. The relative luciferase activities, the ratio of *Firefry* luciferase to *Renilla* luciferase, are shown as luciferase activities in the 293T cells transfected with each set of illustrated vectors (a, b, c, and d) divided by that in the 293T cells transfected with pBIND, pACT and pG5 *luc* (a). (B) Colocalization of the NP of HTNV and Ubc9 in 293T cells. The pEGFP-Ubc9 was transfected into HTNV-infected Vero E6 cells. At 48 h.p.t., cells were fixed and stained with anti-HTN-NP MAb (51). The arrow shows the colocalization signal of EGFP-Ubc9 and HTNV-NP.

Ubc9. The β-Gal activity of each transformant was measured to estimate the binding between the NP and Ubc9 (Fig. 3). The yeast cells cotransformed with pACT2-Ubc9 and pAS2-1-HTN-NPΔ1–33, -Δ1–100, -Δ401–429, -Δ334–429, or -Δ239–429 expressed β-Gal at levels comparable to that expressed in the cells cotransformed with the pAS2-1-HTN-NP (wild-type (wt)-NP) and pACT2-Ubc9 (Fig. 3). On the other hand, the yeast cells co-transformed with pACT2-Ubc9 and pAS2-1-HTNV-NPΔ1–133, -Δ1–166, -Δ1–199, or -Δ169–429 expressed significantly lower levels of β-Gal (Fig. 3). Therefore, the aa residues at the aa positions between 101 and 238 of the NP are thought to be necessary for the interaction with Ubc9.

Interaction between the NP of HTNV and SUMO-1 in yeast cells

Ubc9 is an enzyme that covalently conjugates SUMO-1 at the K residue of the target proteins within the consensus binding motif "(Ψ)-lysine (K)-X-glutamic acid (E)" (38). Therefore, we examined the binding of SUMO-1 with the NP. Recently, Sampson *et al.*, (*38*) reported that the binding consensus sequence motif for Ubc9 and SUMO-1 was "(Ψ)KXE," where Ψ was any highly hydrophobic aa, and X was any aa, respectively. We searched this consensus sequence motif within the NP and found such a motif "methionine (m)-K-alanine (A)-E" at the aa positions between 188 and 191. Other strains of hantaviruses (4, 9, 46, 48) also have one or two binding motifs for Ubc9 and SUMO-1 within the NP (Fig. 3B). This may indicate that the binding of the NP with the Ubc9 and SUMO-1 is a common feature for hantaviruses. We expected the SUMO-1 modification (sumoylation) of the NP of HTNV, because the NP interacts with Ubc9 at the aa positions between 101 and 238, which contains the consensus binding sequence. We constructed the prey vector, pACT2-SUMO-1, as a counterpart of pAS2-1-HTN-NP in the yeast two-hybrids interaction assay to examine the binding between SUMO-1 and the NP. Y190 yeast cells were cotransformed with both vectors and β-Gal activity in the cotransformed cells was measured. As expected, the NP interacted with SUMO-1 in the yeast cells (Fig. 4). However, β-Gal activity in the yeast cells cotransformed with both vectors was lower than that in the cells co-transformed with pAS2-1-HTN-NP and pACT2-Ubc9.

A

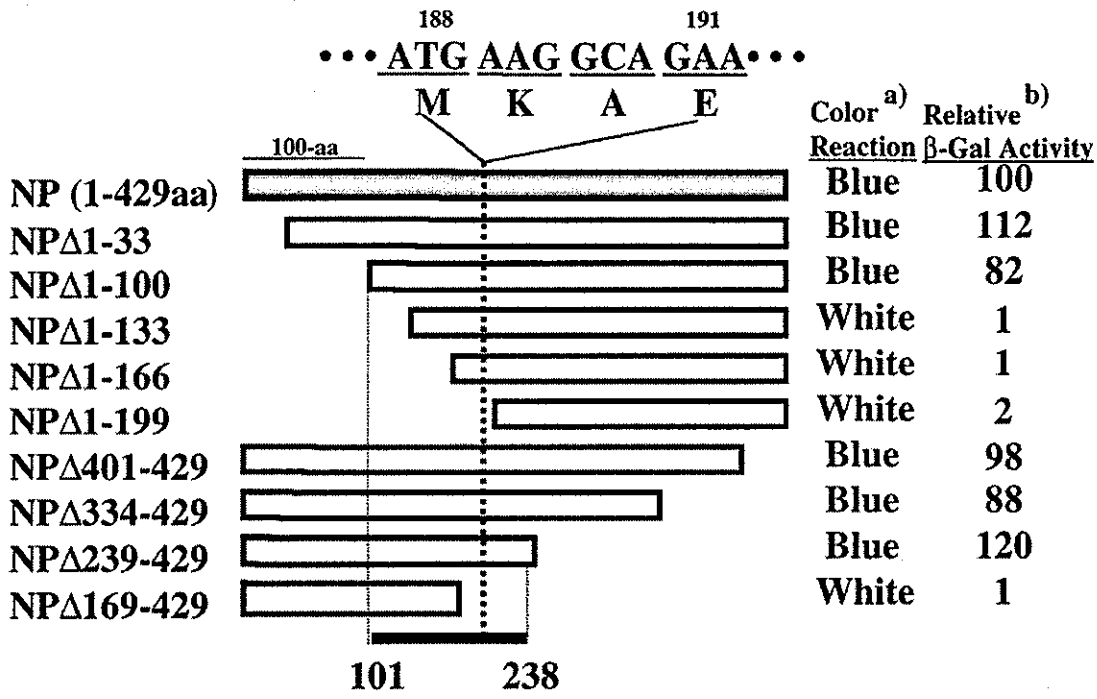

B

Virus	(φ)KXE sequences within the NP	aa-position within the NP
HTNV [1)]	MKAE	188-191
TOPV [2)]	MKAE	188-191
PUUV [3)]	MKAE	188-191
PHV [4)]	MKVE	188-191
	LKAE	247-250
SNV [5)]	LKRE	61-64

FIG. 3. Mapping of the Ubc9 binding sites in the NP of HTNV. (A) A series of deletion mutants of the NP was expressed in yeast cells to determine the Ubc9 binding sites in the NP. The wt-NP consisting of 429-aa is shown at the top. The NPs containing N-terminal deletions; NPΔ1–33, NPΔ1–100, NPΔ1–133, NPΔ1–166 and NPΔ1–199, and the NPs containing C-terminal deletions; NPΔ401–429, NPΔ334–429, NPΔ239–429, NPΔ169–429 are shown in the figure. a) Color reactions were performed by yeast filter assays. When Ubc9 interacts with the mutant NPs, the color of the yeast colonies changes from white to blue as described in the text. b) β-Gal activities were measured by β-Gal assay. The relative β-Gal activities are shown as the β-Gal activity in the yeast expressing the mutant NPs and Ubc9 divided by that in the yeast expressing wt-NP and Ubc9. aa 101–238 of the NP (shown by a thick black bar at bottom) was important for the binding with Ubc9. This region contains the MKAE sequence (aa 188–191) that is one of the common consensus binding motifs ((Ψ)KXE) for SUMO-1 and its conjugating enzyme, Ubc9 (see text). (B) The consensus binding motif in the NP of hantaviruses for Ubc9 and SUMO-1. The consensus sequences in the NP of HTNV (Schumaljohn, C.S., *et al.*, 1986) (41), Topografov virus (TOPV) (Vapalahti, O., *et al.*, 1999) (48), Puumala virus (PUUV) (Escutenaire, S., *et al.*, 2001) (9), Prospect Hill (PHV) (Huang, C., *et al.*, 1996) (15), and Sin Nombre virus (SNV) (Spiropoulou, C.F., *et al.*, 1994) (47) for the interactions with Ubc9 or SUMO-1 are shown in the table. The aa positions of the sequences are shown at the right.

Identification of the interaction site of the NP with Ubc9 or SUMO-1

To define the interaction site of the NP with Ubc9 or SUMO-1, we introduced substitutions at aa 189 (referred to as NP-K189arginine (R) and NP-K189A), at aa 191 (NP-E191A and NP-E191aspartic acid (D)), and at both aa 189 and 191 (NP-K189A/E191A). We also deleted the entire consensus motif (referred to as NPΔ188–191) (Table 1). As expected, β-Gal activity in the yeast cells cotransformed with pAS2-1-HTN-NPΔ188–191 and pACT2-Ubc9 was much lower than that in the yeast cells cotransformed with pAS2-1-HTN-NP and pACT2-Ubc9 (Table 2). This result indicates that Ubc9 binds to the NP at the consensus binding motif "MKAE" at aa 188–191. The substitution of K to R in the motif of the NP (NP-K189R) did not abolish the interaction with Ubc9 *in vivo*. NP-K189R also interacted with SUMO-1 in the yeast system (Table 1), even though the interaction between these two proteins was weaker than that between the wt-NP and SUMO-1. There was a weak interaction between NP-K189A and Ubc9 (Table 1). The substitution of E to D at aa 191 in the NP had no effect on the interaction with

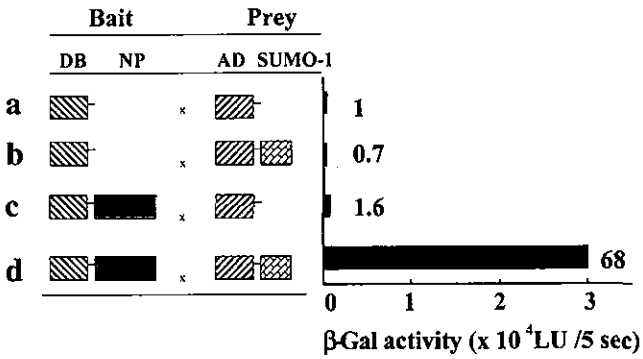

FIG. 4. Interaction between the NP of HTNV and SUMO-1 in yeast cells. Y190 yeast cells were cotransformed with pAS2-1 (control bait vector) and pACT2 (control prey vector) (a), pAS2-1 and pACT2-SUMO-1 (b), pAS2-1-HTN-NP and pACT2 (c), or pAS2-1-HTN-NP and pACT2-SUMO-1 (d). Interactions were measured by β-Gal assay. The bait domain (DB), the NP, the prey domain (AD), and the SUMO-1 are illustrated. The relative β-Gal activities are shown as the β-Gal activity in the yeast cells cotransformed with each of the illustrated vectors divided by that in the yeast cotransformed with pAS2-1 and pACT2 (a).

Ubc9 and SUMO-1 (Table 1). In the case of substitutions of K to A at aa 189 and E to A at aa 191, the interaction between the mutated NPs and Ubc9 were significantly lower than that between the wt-NP and Ubc9 (Table 1). These results indicate that the region from aa 188–191 in the NP of HTNV is responsible for the interaction with Ubc9 and that K residue at aa189 of the NP is crucial for the interaction.

We next examined the subcellular localization of mutant NPs in mammalian cells. Red fluorescent protein (RFP)-tagged wt-NP, NP-K189A, NP-E191A, NP-K189A/E191A, NP-K189R, NP-E191D and NPΔ188–191 were transiently expressed in 293T cells (Fig. 5) or Vero E6 cells (data not shown) by transfection with pDsRed2-HTN-NP, pDsRed2-HTN-NP-K189A, pDsRed2-HTN-NP-E191A, pDsRed2-HTN-NP-K189A/E191A, pDsRed2-HTN-NP-K189R, pDsRed2-HTN-NP-E191D, and pDsRed2-HTN-NPΔ188–191. We found that wt-NP, NP-K189A, NP-E191A, NP-K189A/E191A, NP-K189R, and NP-E191D localized at the perinuclear region, while NPΔ188–191 dispersed into the cytoplasm (Fig. 5, g-2). The mutant-NPs were similarly stable in the transfected cells as estimated by Western blot analysis (data not shown). These results indicate that the difference in subcellular localization of NPΔ188–191 is not due to differences in the stability of the protein, but rather due to the absence of the interaction with SUMO-1.

DISCUSSION

During viral infection, many viral proteins are post-translationally modified by viral or cellular enzymes, through processes such as acetylation (*43*), methylation (34), phosphorylation (*3*, *18*, *33*), glycosylation (*11*, *24*, *36*), ubiquitination (*5*, *10*, *13*) and sumoylation (*1*, *14*, *28*). These modifications may lead to protein-folding or unfolding, viral assembly or disassembly, transportation of the proteins in the infected cells, protein degradation, and protein deaggregation.

Ubc9 covalently conjugates SUMO-1 to the substrates at their internal K residues (sumoylation) (*27*). Sumoylation of the proteins alters the subcellular localization (*27*,

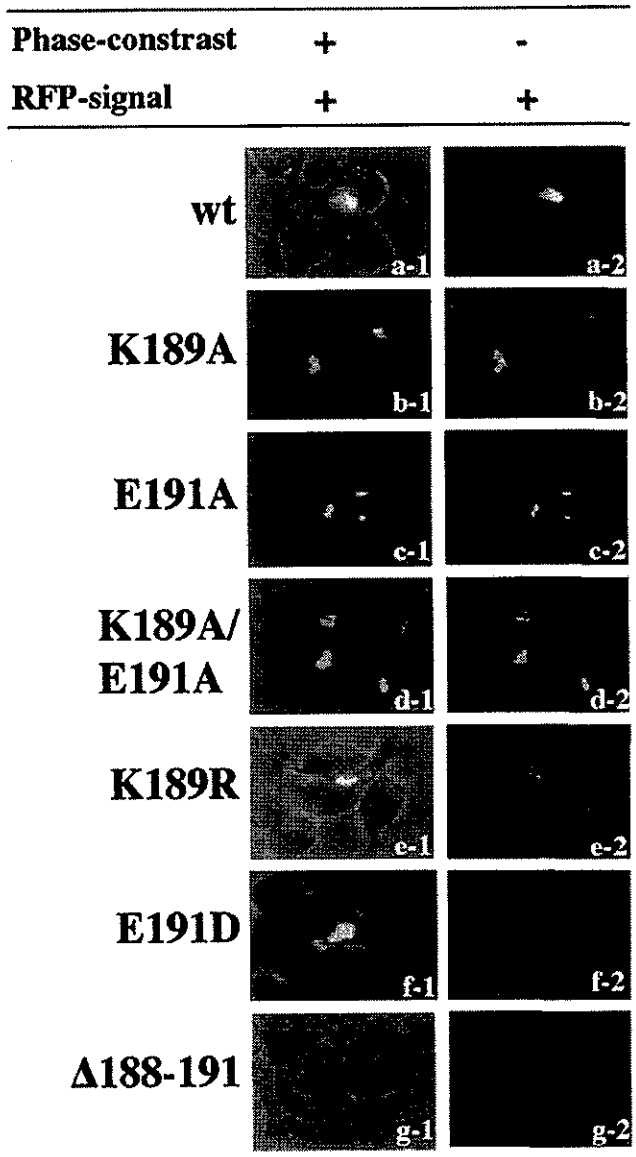

FIG. 5. Subcellular localization of the mutant NPs in living cells. wt-NP (a-1 and a-2), NP-K189A (K189A) (b-1 and b-2), NP-E191A (c-1 and c-2), NP-K189A/E191A (K189A/E191A) (d-1 and d-2) NP-K189R (K189R) (e-1 and e-2), NP-E191D (E191D) (f-1 and f-2), and NPΔ188–191 (Δ188–191) (g-1 and g-2) were expressed as RFP-conjugating forms in 293T cells. pDsRed2-HTN-NP, pDsRed2-HTN-NP-K189A, pDsRed2-HTN-NP-K189A/E191A, pDsRed2-HTN-NP-K189R, pDsRed2-HTN-NP-E191D, and pDsRed2-HTN-NPΔ188–191 were transfected into 293T cells. At 48 h.p.t., the expressed NPs were observed under a immunofluorescence microscopy at with (*left panels*) (a-1, b-1, c-1, d-1, e-1, f-1 and g-1) or without (right panels) (a-2, b-2, c-2, d-2, e-2, f-2, and *g-2*) phase-difference condensation, to see the subcellular localization of the NPs and the red-fluorescence signals (RFP-signals), respectively.

TABLE 1

The Interaction of the NPs with Ubc9 and SUMO-1 in the Yeast Cells

HTNV NPs		Binding with[b]	
NPs	Sequences[a]	Ubc9	SUMO-1
Control[c]	–	–[d]	–[e]
wt-NP	····· AQSSMKAEEIT····	+++	+++
NP-K189A	····· AQSSMAAEEIT ····	+	+
NP-E191A	····· AQSSMKAAEIT ····	+++	++
NP-K189A/E191A	····· AQSSMAAAEIT ····	+	++
NP-K189R	····· AQSSMRAEEIT ····	+++	++
NP-E191D	····· AQSSMKADEIT ····	+++	+++
NP-Δ189–191	····· AQSS EIT ····	–	–

[a] The amino acid sequence corresponding to 184–194 of the wt-NP of HTNV was shown.

[b] β-Gal activities of cotransformed yeast cells with pAS2-1 NPs and pACT2 Ubc9 or pACT2 SUMO-1 were measured by β-Gal assays as described in the text.

[c] The empty vector, pAS2-1, was used as a negative control.

[d] The interactions were scored according to the rate of the negative control (Control) as follows: >30, +++; >20, ++; >10, +; >1; ±; <1; –.

[e] The interactions were scored according to the rate of the negative control (Control) as follows: >12, +++; >8, ++; >4, +; >1; ±; <1; –.

28) and the stability of the protein in cells (6), as well as DNA replication and repair (*25*, *26*).

The present results indicate that the aa 101–238 region in the NP of HTNV is necessary and sufficient for Ubc9-binding. Li *et al.* (*23*) have recently reported the interaction between the NP of Puumala virus (PUUV) and SUMO-1; however, they did not define the region responsible for the interaction nor discuss the significance of the sumoylation of the NP in the PUUV-infected cells. Other hantaviruses also have a consensus Ubc9 and SUMO-1 binding motif in the NP (Fig. 3, B), so the interaction of the NP with Ubc9 and SUMO-1 may be a common feature in hantaviruses.

To define the actual interaction region of the NP with Ubc9 and SUMO-1, the binding consensus motif, MKAE, at aa 188–191 in the NP of HTNV was deleted (NPΔ188–191). As expected, the interaction between the NP and Ubc9 or SUMO-1 was completely abolished (Table 1). Therefore, these 4 amino acids at aa 188–191 appear to be crucial for the interaction between the NP and Ubc9 or SUMO-1. We then constructed several substitution mutants of the NP. A substitution of K to R at aa 189 in the HNTV-NP did not affect the interaction of NP with the Ubc9 but reduced that with SUMO-1. A substitution of K to A at aa 189, however, strongly affected the interaction of the NP with both Ubc9 and SUMO-1. These results suggest that the second amino acid in the motif is basic for binding with Ubc9. Since sumoylation is occurs at the K residue in general, SUMO-1 may indirectly bind the mutant NPs such as NP-K189R and -K189A by binding with the Ubc9 homolog of the yeast cells. Sampson *et al.* (38) reported that the substitution of K to A residue within the binding motif of the RanGAP1 abolished the interaction with both Ubc9 and SUMO-1, while the substitution of K to R abolished the interaction with SUMO-1 but not with Ubc9 in an *in vitro* binding assay system. The discrepancy between their observations and ours may be due to differences in and the sensitivity of the assay system employed or differences in the target proteins analyzed. They also showed that the E residue in the motif of the RanGAP1 is also important. In the present study, the substitution of E to A and E to D at aa 191 of the NP (NP-E191A and NP-E191D, respectively) did not affect the interaction with either Ubc9 or SUMO-1, indicating that the fourth amino acid in the motif is not crucial for the interaction. However, we could not rule out the possibility that E residue at aa 192, the next amino acid residue of the motif, compensated the function of E residue at aa 191 in these mutant NPs.

In the present study, the interaction of the HTNV-NP with Ubc9 or SUMO-1 was not associated with the proteolysis of the NP since the steady-state levels of the mutant NPs in mammalian cells estimated by Western blot analysis were nearly the same as that of the wt-NP. Rather, the differences in the localization patterns among the mutant NPs in the cytoplasm were correlated with the degree of interaction of the NP with Ubc9 or SUMO-1. Thus, the interaction of the NP with Ubc9 or SUMO-1 is likely to be necessary for the proper subcellular localization of the NP. In the case of Black Creek Canal virus (BCCV) (Fig. 1) (*31*), the C-terminal 141-aa residues of the NP have been shown to target the green fluorescent protein to the perinuclear region in the cells. The interaction of the NP with Ubc9 or SUMO-1 might alter the conformation of the NP resulting in exposure of the C-terminal perinuclear targeting sequence.

The C-terminal 93-aa residues of the NP of HTNV and PUUV are reported to be important for the nonspecific RNA binding of the NP (Fig. 1) (*12*). Severson *et al.* (*44*) reported that the HTNV-NP preferentially binds to full-length S-RNA. More recently, Xu *et al.* (*50*) showed that the aa 197–218 region of the HTNV-NP contains the major RNA binding determinants and that the aa 175–196 region contributes to the specificity of viral RNA recognition (Fig. 1). Interestingly, this region overlaps with the binding site of Ubc9 and SUMO-1. It would be of interest to elucidate if the interaction of the NP with Ubc9 or SUMO-1 affects the specificity of viral RNA recognition by the NP.

Using a yeast two-hybrid screening system, Li *et al.* (*23*) found that the PUUV-NP interacts with the Fas-mediated apoptosis enhancer, Daxx, at the C-terminal 57-aa residues in the NP (Fig. 1). They hypothesized that the interaction of the PUUV-NP with Daxx regulated the localization of the NP and was involved in the apoptotic process of the infected cells (*23*). Interestingly, Daxx in-

TABLE 2

Oligonucleotides Used in This Study

No.	Primer name	Sequence	Binding site (protein)	Polarity	Restriction enzymes
#1	HTN NP1*Nco*I	GGCCATGGCAACTATGGAGGAATTAC	1–22 (NP)	+	*Nco*I
#2	*HTN-NP1290Bgl*IIr	GAGATCTTAGAGTTTCAAAGGCTCTTGG	1265–1290 (NP)	–	*Bgl*II
#3	UBC-r477	GCGGATCCTTATGAGGGCGCAAACTTCTTG	456–477 (Ubc9)	–	*Bam*HI
#4	SUMO-1Br	CGGATCCTAAACTGTTGAATGACCCCCCG	274–306 (SUMO-1)	+	*Bam*HI
#5	UBC-f1	GGGATCCGAATGTCGGGGATCGCCCTCAGC	1–21 (Ubc9)	+	*Bam*HI
#6	SUMO-1Bf	GGGATCCACATGTCTGACCAGGAGGCAAAA	1–21 (SUMO-1)	+	*Bam*HI
#7	N-100	GCCATGGATCCAGATGAGTTGAACAAG	103–123 (NP)	+	*Nco*I
#8	N-300	GGCCATGGTGCTGGATTTAAACCATTTGG	301–322 (NP)	+	*Nco*I
#9	N-400	GCCATGGCTCTGTATATGTTGACAACAAGG	409–432 (NP)	+	*Nco*I
#10	*N-500*	GGCCATGGATGTTAACGGTATCCGGAAAC	499–529 (NP)	+	*Nco*I
#11	N-600	GGCCATGGCAGTCTGTGGGCTCTACCCTGC	601–623 (NP)	+	*Nco*I
#12	C-100	GGAGATCTATCCCCTAAGTGGAAGTTGTC	1180–1200 (NP)	–	*Bgl*II
#13	C-400	GGAGATCTAATATCTTCAATCATGCTACAG	876–897 (NP)	–	*Bgl*II
#14	C-600	GGAGATCTACTCCAGTCCTTTGCTAATGC	679–699 (NP)	–	*Bgl*II
#15	HTN NP425f	AACAAGGGGGAGGCAAACTACC	426–447 (NP)	+	
#16	d88-91r	CTATATCTACCAGGTGTAATCTC[a]GCTTGACTGTGCATTTGGCAAG	540–561,574–596 (NP)	–	
#17	d88-91f	CTTGCCAAATGCACAGTCAAGC[b]GAGATTACACCTGGTAGATATAG	540–561,574–596 (NP)	+	
#18	HTN NP747r	GTATCTGGAAGAAGCTTGCAAG	728–749 (NP)	–	
#19	K189Rr	GTAATCTCTTCTGCC[C]TCATGCTTGACTG	543–571 (NP)	–	
#20	K189Rf	CAGTCAAGCATGA[G]GGCAGAAGAGATTAC	543–571 (NP)	+	
#21	K189Ar	GTAATCTCTTCTGCCGCCATGCTTGACTG	543–571 (NP)	–	
#22	K189Af	CAGTCAAGCATG[GC]GGCAGAAGAGATTAC	543–571 (NP)	+	
#23	E191Dr	GTAATCTC[G]TCTGCCTTCATGCTTGACTG	543–571 (NP)	–	
#24	E191Df	CAGTCAAGCATGAAGGCAGA[C]GAGATTAC	543–571 (NP)	+	
#25	E191Ar	GTAATCTCT[G]CTGCCTTCATGCTTGACTG	543–571 (NP)	–	
#26	*E191Af*	CAGTCAAGCATGAAGGCAG[C]AGAGATTAC	543–571 (NP)	+	
#27	K189A/E191Ar	GTAATCTCT[G]C[TGC]TGCCATGCTTGACTG	543–571 (NP)	–	
#28	K189A/E191Af	CAGTCAA[GCA]TGGCAG[C]AGCAGAGATTAC	543–571 (NP)	+	
#29	HTN-NP1-*Xba*I	CCTCTAGAATGGCAACTATGGAGGAATTAC	1–22 (NP)	+	*Xba*I
#30	HTN-NP1290-*Kpn*I	CCGGTACCTTAGAGTTTCAAAGGCTCTTG	1266–1290 (NP)	–	*Kpn*I
#31	UBC9f1-*Bam*HI	CCGGATCCATGTCGGGGATCGCCCTCAGC	1–21 (Ubc9)	+	*Bam*HI

[a]: The sequence, TTCTGCCTTCAT, was deleted from the anti-sense sequence of the NP at 540 to 596-nt.
[b]: The sequence, ATGAAGGCAGAA, was deleted from the sense sequence of the NP at 540 to 596-nt.
□: Mutations were introduced in the boxed sequences.

teracts with Ubc9 and is covalently conjugated with SUMO-1 in 293T cells (*16*, *37*). Thus, it might be possible that the complex of NP-Ubc9-SUMO-1-Daxx regulates the subcellular localization of the HTNV-NP. Another report indicated that the actin microfilament plays an important role in viral assembly in the BCCV-infected cells (Fig. 1) (*32*). It is necessary to clarify how these cellular factors are involved in the assembly of the NP and whether these factors affect independently or cooperatively in the assembly process.

MATERIALS AND METHODS

Virus and cells

The 76–118 strain of HTNV (*41*) was used in the study. Virus propagation and titration in Vero E6 cells were carried out as described previously (41). Vero E6 and 293T cells were grown in Doulbeco's modified minimum essential medium (DMEM, GIBCO BRL) containing 5% fetal calf serum (FCS) and 60 mg/ml of kanamycin.

Primers

The primers used for a polymerase chain reaction (PCR) are listed in Table 2.

Yeast two-hybrid screening and interaction assay

The yeast two-hybrid bait plasmid, pAS2–1 (CLONTECH, Lab., Inc.), containing a cDNA of the open reading frame (ORF) of the NP (referred to as pAS2–1-HTN-NP) was constructed as follows. PCR was performed with pGEM1-HTN-S (41) as a template and primers #1 and #2 using a High-fidelity PCR Kit (Roche). The PCR product was cloned into the pGEM*Teasy vector* (Promega, referred to as pGEM-HTN-NP) and the sequence of the insert was confirmed to be identical to the original sequence. pGEM-HTN-NP was digested with restriction enzymes *Nco*I and *Bgl*II, and the digested DNA fragment containing the ORF of the NP was inserted into the *Nco*I and *Bam*HI sites of pAS2–1 (pAS2–1-HTN-NP).

We used a cDNA library of HeLa cells cloned into

pACT2, pACT2-HeLa-cDNA library (CLONTECH, Lab., Inc.), consisting of 1×10^6 independent clones of the screening targets against the NP. We used the yeast two-hybrid Kit (CLONTECH, Lab., Inc.) to screen the library according to the manufacturer's instructions. Briefly, we cotransformed yeast Y190 cells with pAS2-1-HTN-NP and pACT2-HeLa-cDNA library and then selected the transformants on the yeast growing plates depleted by three nutritions: tryptophan and leucine as the selectable markers of the transformants of pAS2-1 and pACT2 vectors, respectively, and histidine as the interaction marker. To estimate the protein-protein interactions in the yeast cells, we employed a filter lift assay, a standard protocol to detect *lac*Z-expression using 5-bromo-4-chloro-3-indolyl-β-D-galactopyranoside (X-Gal), or a β-Gal assay (Galacto-Light, TROPIX, M.A., U.S.A.) to quantify the β-Gal activity. For the β-Gal assay, the yeast cells (2×10^6 cells) were frozen and thawed, and mixed with a reaction buffer containing Galacton as a substrate. The reaction mixture was incubated at room temperature for one hour and then the acceleration solution was added to the mixture. Light Units (LU) per 5 sec (s) were counted by a luminometer (Microtech NITI-ON, Inc., Japan). All the media and reagents for yeast culture were purchased from CLONTECH, Lab., Inc.

Analysis of the interaction between HTNV-NP and Ubc9 or SUMO-1 in yeast cells.

The cDNAs of Ubc9 and SUMO-1 were synthesized from mRNAs extracted from HeLa cells by reverse transcription reaction using primers #3 and #4, respectively. The cDNAs were amplified by PCR using primers #5 and #3, #6 and #4, respectively. The PCR products were digested with a restriction enzyme, *Bam*HI, and cloned into the *Bam*HI site of a prey vector, pACT2, for a sense direction (referred to as pACT2-Ubc9 and pACT2-SUMO-1, respectively).

A series of deletion mutations were introduced into the NP gene by the PCR-based procedure. PCRs were performed using pGEM-HTN-NP as a template and each of the following sets of primers; #7 and #2 for pAS2-1-HTN-NPΔ1–30, #8 and #2 for pAS2-1-HTN-NPΔ1–100, #9 and #2 for pAS2-1-HTN-NPΔ1–133, #10 and #2 for pAS2-1-HTN-NPΔ1–166, #11 and #2 for pAS2-1-HTN-NPΔ1–199, #1 and #12 for pAS2-1-HTN-NPΔ401–429, #1 and #13 for pAS2-1-HTN-NPΔ334–429, and #1 and #14 for pAS2-1-HTN-NPΔ239–429. Each PCR product was digested with restriction enzymes, *Nco*I and *Bgl*II, and cloned into the *Nco*I and *Bam*HI sites of pAS2-1. To construct the HTN-NPΔ169–429 expression vector, pAS2-1-HTN-NPΔ169–429, the PCR fragment amplified with primers #1 and #2 was digested with restriction enzymes, *Nco*I and *Hpa*I, and then the small DNA fragment was cloned into the *Nco*I and *Sma*I site of pAS2-1.

To introduce a 4-aa deletion, MKAE, at the aa position between 188 and 191, recombinant PCRs were performed. First PCRs were performed using primers #15 and #16, #17 and #18 and pGEM-HTN-NP as a template. Subsequent PCRs were carried out using primers #15 and #18 as primers, and #15/#16 and #17/#18 products as templates. The PCR product was digested with restriction enzymes, *Hpa*I and *Hin*dIII, and then used to replace the same region of the pGEM-HTN-NP at the *Hpa*I and *Hin*dIII sites (referred to as pGEM-HTN-NPΔ188–191). The mutated HTNV-NP fragment was separated from pGEM-HTN-NPΔ188–191 by digestion with restriction enzymes, *Nco*I and *Bgl*II, and cloned into the *Nco*I and *Bam*HI sites of pAS2-1 to construct pAS2-1-HTN-NPΔ188–191. pGEM-HTN-NP and pAS2-1-HTN-NP containing a substitution mutation, K to R at aa 189 (referred to as pGEM-HTN-NP-K189R and pAS2-1-HTN-NP-K189R), K to A at aa 189 (referred to as pGEM-HTN-NP-K189A and pAS2-1-HTN-NP-K189A), E to D at aa 191 (referred to as pGEM-HTN-NP-E191D and pAS2-1-HTN-NP-E191D), E to A at aa 191 (referred to as pGEM-HTN-NP-E191A and pAS2-1-HTN-NP-E191A), and K to A at aa 189/E to A at aa 191 (referred to as pGEM-HTN-NP-K189A/E191A and pAS2-1-HTN-NP-K189A/E191A) were similarly constructed using primers #15, #19, #20 and #18; #15, #21, #22 and #18; # 15, #23, #24 and #18; # 15, #25, #26 and #18; and; # 15, #27, #28 and #18, respectively, in recombinant PCRs.

Mammalian two-hybrid interaction assay

To demonstrate the interaction between the HTNV-NP and Ubc9 in mammalian cells, mammalian two-hybrid plasmids were constructed. To construct a bait vector, pBIND-HTN-NP, the PCR product of the NP amplified using primers #29 and #30, was digested with restriction enzymes, *Xba*I and *Kpn*I, and inserted into the *Xba*I and *Kpn*I site of a bait plasmid, pBIND (Promega). To construct a prey vector, pACT-Ubc9, the PCR product of Ubc9 amplified using primers #3 and #5 was digested with *Bam*HI and then inserted into the *Bam*HI site of a prey plasmid, pACT (Promega), for a sense direction (referred to as pACT-Ubc9).

To examine the protein-protein interactions in mammalian cells, 293T or Vero E6 cells were transiently transfected with 3 mammalian two-hybrid vectors, a pBIND construct, a pACT construct and pG5*luc* vectors (CheckMate Mammalian Two-Hybrid System, Promega) using FuGENE6 transfection reagent (Roche). When two proteins expressed from the pBIND and pACT constructs interact with each other, the *Firefry* luciferase encoded in pG5*luc* should be expressed through the activation of its promoter. Additionally, we examined transfection efficiency by monitoring the expression of *Renilla* luciferase as an internal marker, which is encoded in the pBIND vector and is expressed under the control of a human cytomegalovirus immediate-early (CMV-IE) promoter in

the transfected cells. We normalized the protein-protein interactions in mammalian cells by the formula: Interaction units (ratio) = LU obtained from *Firefry* luciferase/LU obtained from *Renilla* luciferase Luciferase activities were measured by the luciferase assay system (Dual-Luciferase Reporter Assay System, Promega) according to the manufacturer's instructions. Briefly, the cells were harvested and lysed at 48 h post transfection (h.p.t.), and the lysates were mixed with LARII reagent. The activities of *Firefry* luciferase were measured for 30 s. STOP & Glo reagent was then added to the reactions and the activity of *Renilla* luciferase was immediately measured for 30 s.

Analysis of subcellular localization of the NP and Ubc9 in mammalian cells

A vector, pEGFP-C1-Ubc9, to express a fusion protein of EGFP and Ubc9, was constructed as follows. The cDNA of Ubc9 was amplified using primers #31 and #3 and the PCR product was digested with *Bam*HI and then inserted into the *Bam*HI site of a pEGFP-C1 plasmid-(CLONTECH, Lab., Inc.). To construct vectors expressing the wt- and mutant-NPs tagged with RFP, pGEM-HTN-NP, pGEM-HTN-NPΔ188–191, pGEM-HTN-NP-K189A, pGEM-HTN-NP-K189R, pGEM-HTN-NP-E191A, pGEM-HTN-NP-E191D, and pGEM-HTN-NP-K189A/E191A were digested with *Nco*I and filled-in using a Klenow fragment of DNA polymerase I, and then digested with *Bgl*II. The fragments containing wt- and mutant-NPs were purified and inserted into the *Sma*I and *Bam*HI site of the pDsRed2-C1 vector (CLONTECH, Lab., Inc.), referred to as pDsRed2-HTN-NP for a wt-NP, pDsRed2-HTN-NPΔ188–191, pDsRed2-HTN-NP-K189A, pDsRed2-HTN-NP-K189R, DsRed2-HTN-NP-E191A, pDsRed2-HTN-NP-E191D, and pDsRed2-HTN-NP-K189A/E191A for mutant NPs, respectively.

The cells transfected with the expression vectors or the HTNV-infected cells were fixed in a mixture of 50% methanol and 50% acetone. The fixed cells were reacted with a monoclonal antibody (MAb) against the NP of HTNV, C16D11 (51), at a dilution of 1:200. The cells were then reacted with a rhodamine-conjugated anti-mouse IgG antibody (Zymed) and examined for staining pattern under a immunofluorescence microscope (Zeiss, HBO50/AC, Germany).

293T or Vero E6 cells were transfected with the vectors for expressing the RFP-tagged NPs using FuGENE6 transfection reagent. After 48 h.p.t., the subcellular localization of the expressed proteins was monitored without fixation under a immunofluorescence microscope (Olympus, CK40, Japan) .

ACKNOWLEDGMENTS

We thank Ms. M. Ogata for her assistance and Dr. J. Maeda of The Institute of Medical Science, The University of Tokyo, for her careful proofreading of this paper. This study was supported by grants from the Ministry of Health, Welfare, and Labour and the Ministry of Education, Science, Culture and Sports of Japan.

REFERENCES

1. Ahn, J. H., Y. Xu, W. J. Jang, M. J. Matunis, and G. S. Hayward. (2001). Evaluation of interactions of human cytomegalovirus immediate-early IE2 regulatory protein with small ubiquitin-like modifiers and their conjugation enzyme Ubc9. *J. Virol.* **75,** 3859–3872.
2. Alfadhli, A., Z. Love, B. Arvidson, J. Seeds, J. Willey, and E. Barklis. (2001). Hantavirus nucleocapsid protein oligomerization. *J. Virol.* **75,** 2019–2023.
3. Arrese, M., and A. Portela. (1996). Serine 3 is critical for phosphorylation at the N-terminal end of the nucleoprotein of influenza virus A/Victoria/3/75. *J. Virol.* **70,** 3385–3391.
4. Botten, J., K. Mirowsky, D. Kusewitt, M. Bharadwaj, J. Yee, R. Ricci, R. M. Feddersen, and B. Hjelle. (2000). Experimental infection model for Sin Nombre hantavirus in the deer mouse (Peromyscus maniculatus). *Proc. Natl. Acad. Sci. USA* **97,** 10578–10583.
5. Bultmann, A., J. Eberle, and J. Haas. (2000). Ubiquitination of the human immunodeficiency virus type 1 env glycoprotein. *J. Virol.* **74,** 5373–5376.
6. Buschmann, T., S. Y. Fuchs, C. G. Lee, Z. Q. Pan, and Z. Ronai. (2000). SUMO-1 modification of Mdm2 prevents its self-ubiquitination and increases Mdm2 ability to ubiquitinate p53. *Cell* **101,** 753–762.
7. Cosgriff, T. M. (1991). Mechanisms of disease in Hantavirus infection: Pathophysiology of hemorrhagic fever with renal syndrome. *Rev. Infect. Dis.* **13,** 97–107.
8. Duchin, J. S., F. T. Koster, C. J. Peters, G. L. Simpson, B. Tempest, S. R. Zaki, T. G. Ksiazek, P. E. Rollin, S. Nichol, E. T. Umland, and et al. (1994). Hantavirus pulmonary syndrome: A clinical description of 17 patients with a newly recognized disease. *The Hantavirus Study Group. N. Eng.l J. Med.* **330,** 949–955.
9. Escutenaire, S., P. Chalon, P. Heyman, G. Van der Auwera, G. van der Groen, R. Verhagen, I. Thomas, L. Karelle-Bui, A. Vaheri, P. P. Pastoret, and A. Plyusnin. (2001). Genetic characterization of Puumala hantavirus strains from Belgium: Evidence for a distinct phylogenetic lineage. *Virus Res.* **74,** 1–15.
10. Everett, R. D. (2000). ICP0 induces the accumulation of colocalizing conjugated ubiquitin. *J. Virol.* **74,** 9994–10005.
11. Gagneten, S., O. Gout, M. Dubois-Dalcq, P. Rottier, J. Rossen, and K. V. Holmes. (1995). Interaction of mouse hepatitis virus (MHV) spike glycoprotein with receptor glycoprotein MHVR is required for infection with an MHV strain that expresses the hemagglutinin-esterase glycoprotein. *J. Virol.* **69,** 889–895.
12. Gott, P., R. Stohwasser, P. Schnitzler, G. Darai, and E. K. Bautz. (1993). RNA binding of recombinant nucleocapsid proteins of hantaviruses. *Virology* **194,** 332–337.
13. Harty, R. N., M. E. Brown, J. P. McGettigan, G. Wang, H. R. Jayakar, J. M. Huibregtse, M. A. Whitt, and M. J. Schnell. (2001). Rhabdoviruses and the cellular ubiquitin-proteasome system: A budding interaction. *J. Virol.* **75,** 10623–10629.
14. Hofmann, H., S. Floss, and T. Stamminger. (2000). Covalent modification of the transactivator protein IE2-p86 of human cytomegalovirus by conjugation to the ubiquitin-homologous proteins SUMO-1 and hSMT3b. *J. Virol.* **74,** 2510–2524.
15. Huang, C., W. P. Campbell, R. Means, and D. M. Ackman. (1996). Hantavirus S RNA sequence from a fatal case of HPS in New York. *J. Med. Viro.l* **50,** 5–8.
16. Jang, M.-S., Ryu, S.-W., and Kim, E. (2002). Modification of Daxx by small ubiquitin-related modifier-1. *Biochem. Biophys. Res. Commun.* **295,** 495–500.
17. Jin, H., and R. M. Elliott. (1993). Characterization of Bunyamwera virus S RNA that is transcribed and replicated by the L protein expressed from recombinant vaccinia virus. *J. Virol.* **67,** 1396–1404.

18. Kaptur, P. E., B. J. McCreedy, Jr., and D. S. Lyles. (1992). Sites of in vivo phosphorylation of vesicular stomatitis virus matrix protein. *J. Virol.* **66**, 5384–5392.
19. Kim, K. H., and S. Makino. (1995). Two murine coronavirus genes suffice for viral RNA synthesis. *J. Virol.* **69**, 2313–2321.
20. Kingsbury, D. W. (1974). The molecular biology of paramyxoviruses. *Med. Microbiol. Immunol. (Berl.)* **160**, 73–83.
21. Kruger, D. H., R. Ulrich, and A. A. Lundkvist. (2001). Hantavirus infections and their prevention. *Microbes. Infect.* **3**, 1129–1144.
22. Lee, K. J., I. S. Novella, M. N. Teng, M. B. Oldstone, and J. C. de La Torre. (2000). NP and L proteins of lymphocytic choriomeningitis virus (LCMV) are sufficient for efficient transcription and replication of LCMV genomic RNA analogs. *J. Virol.* **74**, 3470–3477.
23. Li, X.-D., T. P. Makela, D. Guo, R. Soliymani, V. Koistinen, O. Vapalahti, A. Vaheri, and H. Lankinen. (2002). Hantavirus nucleocapsid protein interacts with the Fas-mediated apoptosis enhancer Daxx. *J. Gen. Virol.* **83**, 759–766.
24. Liu, C. K., G. Wei, and W. J. Atwood. (1998). Infection of glial cells by the human polyomavirus JC is mediated by an N-linked glycoprotein containing terminal alpha(2–6)-linked sialic acids. *J. Virol.* **72**, 4643–4649.
25. Mao, Y., M. Sun, S. D. Desai, and L. F. Liu. (2000). SUMO-1 conjugation to topoisomerase I: A possible repair response to topoisomerase-mediated DNA damage. *Proc. Natl. Acad. Sci. USA* **97**, 4046–4051.
26. Matunis, M. J., E. Coutavas, and G. Blobel. (1996). A novel ubiquitin-like modification modulates the partitioning of the Ran-GTPase-activating protein RanGAP1 between the cytosol and the nuclear pore complex. *J. Cell. Biol.* **135**, 1457–1470.
27. Melchior, F. (2000). SUMO–nonclassical ubiquitin. *Annu. Rev. Cell. Dev. Biol.* **16**, 591–626.
28. Muller, S., and A. Dejean. (1999). Viral immediate-early proteins abrogate the modification by SUMO-1 of PML and Sp100 proteins, correlating with nuclear body disruption. *J. Virol.* **73**, 5137–5143.
29. Nichol, S. T. (2001). Bunyaviruses. *In* "Fields Virology," vol. 2 (D. M. Knipe and P. M. Howley, Eds.), pp. 1603–1633. Lippincott Williams & Wilkins, Philadelphia.
30. Osborne, J. C., and R. M. Elliott. (2000). RNA binding properties of bunyamwera virus nucleocapsid protein and selective binding to an element in the 5′ terminus of the negative-sense S segment. *J. Virol.* **74**, 9946–9952.
31. Ravkov, E. V., and R. W. Compans. (2001). Hantavirus nucleocapsid protein is expressed as a membrane-associated protein in the perinuclear region. *J. Virol.* **75**, 1808–1815.
32. Ravkov, E. V., S. T. Nichol, C. J. Peters, and R. W. Compans. (1998). Role of actin microfilaments in Black Creek Canal virus morphogenesis. *J. Virol.* **72**, 2865–2870.
33. Reed, K. E., J. Xu, and C. M. Rice. (1997). Phosphorylation of the hepatitis C virus NS5A protein in vitro and in vivo: Properties of the NS5A-associated kinase. *J. Virol.* **71**, 7187–7197.
34. Rho, J., S. Choi, Y. R. Seong, J. Choi, and D. S. Im. (2001). The arginine-1493 residue in QRRGRTGR1493G motif IV of the hepatitis C virus NS3 helicase domain is essential for NS3 protein methylation by the protein arginine methyltransferase 1. *J. Virol.* **75**, 8031–8044.
35. Richmond, K. E., K. Chenault, J. L. Sherwood, and T. L. German. (1998). Characterization of the nucleic acid binding properties of tomato spotted wilt virus nucleocapsid protein. *Virology* **248**, 6–11.
36. Richt, J. A., T. Furbringer, A. Koch, I. Pfeuffer, C. Herden, I. Bause-Niedrig, and W. Garten. (1998). Processing of the Borna disease virus glycoprotein gp94 by the subtilisin-like endoprotease furin. *J. Virol.* **72**, 4528–4533.
37. Ryu, S.-W., Chae, S.-K., and Kim, E. (2000). Interaction of Daxx, a Fas binding protein, with Sentrin and Ubc9. *Biochem. Biophys. Res. Commun.* **279**, 6–10.
38. Sampson, D. A., M. Wang, and M. J. Matunis. (2001). The small ubiquitin-like modifier-1 (SUMO-1) consensus sequence mediates Ubc9 binding and is essential for SUMO-1 modification. *J. Biol. Chem.* **276**, 21664–21669.
39. Schmaljohn, C. S. (1990). Nucleotide sequence of the L genome segment of Hantaan virus. *Nucleic Acids Res.* **18**, 6728.
40. Schmaljohn, C. S., and J. W. Hooper. (2001). Bunyaviridae: The viruses and their replication., *In* "Fields Virology," vol. 2 (D. M. Knipe and P. M. Howley, Eds.), pp. 1581–1602. Lippincott Williams & Wilkins, Philadelphia.
41. Schmaljohn, C. S., G. B. Jennings, J. Hay, and J. M. Dalrymple. (1986). Coding strategy of the S genome segment of Hantaan virus. *Virology* **155**, 633–643.
42. Schmaljohn, C. S., A. L. Schmaljohn, and J. M. Dalrymple. (1987). Hantaan virus M RNA: coding strategy, nucleotide sequence, and gene order. *Virology* **157**, 31–39.
43. Schneider, P. A., C. G. Hatalski, A. J. Lewis, and W. I. Lipkin. (1997). Biochemical and functional analysis of the Borna disease virus G protein. *J. Virol.* **71**, 331–336.
44. Severson, W., L. Partin, C. S. Schmaljohn, and C. B. Jonsson. (1999). Characterization of the Hantaan nucleocapsid protein-ribonucleic acid interaction. *J. Biol. Chem.* **274**, 33732–33739.
45. Severson, W. E., X. Xu, and C. B. Jonsson. (2001). cis-Acting signals in encapsidation of Hantaan virus S-segment viral genomic RNA by its N protein. *J. Virol.* **75**, 2646–2652.
46. Song, W., N. Torrez-Martinez, W. Irwin, F. J. Harrison, R. Davis, M. Ascher, M. Jay, and B. Hjelle. (1995). Isla Vista virus: A genetically novel hantavirus of the California vole Microtus californicus. *J. Gen. Virol.* **76**, 3195–3199.
47. Spiropoulou, C. F., S. Morzunov, H. Feldmann, A. Sanchez, C. J. Peters, and S. T. Nichol. (1994). Genome structure and variability of a virus causing hantavirus pulmonary syndrome. *Virology* **200**, 715–723.
48. Vapalahti, O., A. Lundkvist, V. Fedorov, C. J. Conroy, S. Hirvonen, A. Plyusnina, K. Nemirov, K. Fredga, J. A. Cook, J. Niemimaa, A. Kaikusalo, H. Henttonen, A. Vaheri, and A. Plyusnin. (1999). Isolation and characterization of a hantavirus from Lemmus sibiricus: Evidence for host switch during hantavirus evolution. *J. Virol.* **73**, 5586–5592.
49. Watanabe, T. K., T. Fujiwara, A. Kawai, F. Shimizu, S. Takami, H. Hirano, S. Okuno, K. Ozaki, S. Takeda, Y. Shimada, M. Nagata, A. Takaichi, E. Takahashi, Y. Nakamura, and S. Shin. (1996). Cloning, expression, and mapping of UBE2I, a novel gene encoding a human homologue of yeast ubiquitin-conjugating enzymes which are critical for regulating the cell cycle. *Cytogenet. Cell. Genet.* **72**, 86–89.
50. Xu, X., W. Severson, N. Villegas, C. S. Schmaljohn, and C. B. Jonsson. (2002). The RNA binding domain of the Hantaan virus N protein maps to a central, conserved resion. *J. Virol.* **76**, 3301–3308.
51. Yoshimatsu, K., J. Arikawa, M. Tamura, R. Yoshida, A. Lundkvist, B. Niklasson, H. Kariwa, and I. Azuma. (1996). Characterization of the nucleocapsid protein of Hantaan virus strain 76–118 using monoclonal antibodies. *J. Gen. Virol.* **77**, 695–704.

ELSEVIER

Journal of Virological Methods 108 (2003) 111–116

Journal of Virological Methods

www.elsevier.com/locate/jviromet

Detection of immunoglobulin G to Crimean-Congo hemorrhagic fever virus in sheep sera by recombinant nucleoprotein-based enzyme-linked immunosorbent and immunofluorescence assays

Tang Qing [a], Masayuki Saijo [b], Han Lei [a], Masahiro Niikura [b], Akihiko Maeda [b], Tetsuro Ikegami [b], Wang Xinjung [c], Ichiro Kurane [b], Shigeru Morikawa [b,*]

[a] *Second Division of Viral Hemorrhagic Fever, Institute of Epidemiology and Microbiology, Chinese Academy of Preventive Medicine, Changping, Beijing 102206, PR China*

[b] *Department of Virology 1, Special Pathogens Laboratory, National Institute of Infectious Diseases, 4-7-1 Gakuen, Musashimurayama, Tokyo 208-0011, Japan*

[c] *Anti-epidemic Station of Shandong Province, 72 Jingshi Road, Jinan 250014, Shandong, PR China*

Received 19 September 2002; received in revised form 13 November 2002; accepted 14 November 2002

Abstract

Crimean-Congo hemorrhagic fever virus is a tick-borne virus that causes severe hemorrhagic symptoms with an up to 50% mortality rate in humans. Wild and domestic animals, such as sheep, cattle and goats, are the reservoirs. The recombinant nucleoprotein-based Crimean-Congo hemorrhagic fever virus antibody detection systems for sheep sera were developed by enzyme-linked immunosorbent assay (ELISA) and an indirect immunofluorescence assay techniques. The samples used for evaluation were 80 sera collected from sheep in a Crimean-Congo hemorrhagic fever-endemic area (western part of the Xinjiang Uygur Autonomous Region) and 39 sera collected from sheep in a disease-free region (Shandong province, eastern China). The ELISA and indirect immunofluorescence assay using recombinant nucleoprotein of the virus proved to have high sensitivity and specificity for detecting the immunoglobulin G antibodies to the virus in sheep sera. Within this limited number of samples, the recombinant nucleoprotein-based ELISA and indirect immunofluorescence assay are considered to be useful tools for seroepidemiological study of virus infections in sheep sera.

Keywords: Crimean-Congo hemorrhagic fever virus; Recombinant nucleoprotein; ELISA; Immunofluorescence; Seroepidemiology

1. Introduction

Crimean-Congo hemorrhagic fever virus belongs to the family Bunyaviridae (genus *Nairovirus*) and causes severe hemorrhagic symptoms in humans (Gonzalez-Scarano and Nathanson, 1996). The disease is prevalent from Africa through Eastern Europe, the Middle East, and Central Asia, to the western part of China (Hoogstraal, 1979). The virus is a tick-borne virus, which is transmitted by ticks of the *Hyalomma* genus (Gonzalez-Scarano and Nathanson, 1996). Humans are usually infected with the virus either by bites from infected ticks or by direct contact with virus-contaminated tissues or blood. Outbreaks of the infection have been reported among abattoir and agricultural workers and shepherds, who handle livestock animals such as sheep, goats and cattle (Khan et al., 1997; Swanepoel et al., 1985). Based on the fact that sheep are one of the sources of Crimean-Congo hemorrhagic fever outbreaks in humans, seroepidemiological studies on virus infections in sheep are important not only for the prevention of Crimean-Congo hemorrhagic fever outbreaks but also for the demarcation of the prevalence of this virus. However, there are two problems facing seroepidemiological studies in sheep. One is the danger of handling live Crimean-Congo hemorrhagic fever virus in the preparation of antigens, and the other is a strong non-

* Corresponding author. Tel.: +81-42-561-0771x791; fax: +81-42-561-2039.
E-mail address: morikawa@nih.go.jp (S. Morikawa).

0166-0934/02/$ - see front matter © 2002 Elsevier Science B.V. All rights reserved.
PII: S0166-0934(02)00267-7